

**Palacký University Olomouc, Faculty of Science,  
Department of Geoinformatics**

**Paris Lodron University Salzburg, Faculty of Natural Sciences,  
Department of Geoinformatics**

**MAPPING MANGROVE FORESTS:  
PROCESSING AND VISUALIZATION OF  
MULTI-SENSOR EARTH OBSERVATION DATA  
FOR THE COLOMBIAN PACIFIC COAST**

**Diploma thesis**

Author

**Sayana DE GOROSTIZAGA MOXON**

Supervisor (Palacký University Olomouc)  
Mgr. Rostislav NÉTEK (Ph.D)

Co-supervisor (Paris Lodron University Salzburg)  
Assoc. Prof. Dirk TIEDE (Ph.D)

**Erasmus Mundus Joint Master Degree Programme  
Copernicus Master in Digital Earth  
Specialization Track Geovisualization & Geocommunication  
Olomouc, Czech Republic, 2021**



Palacký University  
Olomouc



# **ANOTATION**

Mangrove forests are among the most productive ecosystems on Earth and are essential for the preservation of biodiversity and the livelihoods of coastal communities around the world. However, they are facing severe threats from anthropogenic activities, which are having an impact on them both in a direct (human development, pollution, etc) and indirect (sea level rise, changing climatic conditions, etc) form. Remote sensing has become an essential instrument to monitor mangrove forest distributions and land use/cover dynamics within and around these ecosystems. The technological advancements in cloud-computing services such as the Google Earth Engine (GEE), are helping reduce the practical limitations concerning processing power and data availability. This study makes use of data acquired by the Copernicus Sentinel-1 (radar) and Sentinel-2 (optical) missions and combines it with the capabilities of GEE and state-of-the-art classification approaches to derive mangrove forest distributions along the Colombian Pacific coast. The results demonstrate its application and value to uncover the distribution of mangrove forests in a tropical region, where cloud-prevalence poses a common limitation to using optical imagery alone. The findings reveal the distribution and extent of mangrove cover over the entire Colombian Pacific coast for the year 2020. The study contributes to a growing body of research advocating full exploitation of the Copernicus Sentinel-1 and Sentinel-2 imagery in optimizing land cover classification and demonstrates its use for mangrove forest monitoring.

## **KEYWORDS**

Sentinel 1; Sentinel 2; data fusion; forest monitoring; mangrove forests; remote sensing; satellite earth observation; time series analysis; Colombia

Number of pages: 68

Number of appendixes: 3

This thesis has been composed by Sayana de Gorostizaga Moxon for the Erasmus Mundus Joint Master's Degree Program in Copernicus Master in Digital Earth for the academic year 2020/2021 at the Department of Geoinformatics, Faculty of Natural Sciences, Paris Lodron University Salzburg, and Department of Geoinformatics, Faculty of Science, Palacký University Olomouc.

Hereby, I declare that this piece of work is entirely my own, the used references have been acknowledged and the thesis has not been previously submitted to the fulfilment of the higher degree.

20. 05. 2021, Olomouc

Sayana de Gorostizaga Moxon

*I would like to thank my supervisors Mgr. Rostislav Nėtek (Ph.D) (Palacký University) and Assoc. Prof. Dirk Tiede (Ph.D (Paris Lodron University) for the support during the elaboration of my research topic.*

*I would also like to thank Aurelie Shapiro (WWF-Germany) for introducing me to the topic and sharing her work. Finally, I thank Gustavo Castellanos-Galindo for the field data and local insight he provided to this study.*

## ASSIGNMENT OF DIPLOMA THESIS

(project, art work, art performance)

Name and surname: **Sayana DE GOROSTIZAGA MOXON**  
Personal number: **R190790**  
Study programme: **N0532A330010 Geoinformatics and Cartography**  
Field of study: **Geoinformatics and Cartography**  
Work topic: **Mapping Mangrove Forests: Processing and visualization of multi-sensor Earth Observation data for the Colombian Pacific coast**  
Assigning department: **Department of Geoinformatics**

### Theses guidelines

The aim of this study is to process multi-sensor Earth Observation data for mangrove forest cover mapping and integrate the resulting products into a web-map. The pilot study will implement data from Copernicus (Sentinel) missions. The study area will be located in the Colombian Pacific coast. The student will investigate, evaluate and apply techniques for semi-automatic classification and validation, primarily within Google Earth Engine. Finally, the resulting products will be integrated in a web-map used to visualize the map outputs.

The student will attach all the collected datasets and all products of the thesis in digital form. The student will create a website about the thesis following the rules available on the department's website and a poster about the diploma thesis in A2 format. The student will submit the entire text (text, attachments, poster, outputs, input and output data) in digital form on a storage medium and the text of the thesis in two bound copies to the secretary of the department.

Extent of work report: **max 50 pages**  
Extent of graphics content: **as needed**  
Form processing of diploma thesis: **printed**  
Language of elaboration: **English**

#### Recommended resources:

Google Earth Engine.[online] Available from URL: <https://earthengine.google.com/>

Shapiro, Aurelie. (2018). Mozambique Mangrove Extent 1995-present. 10.13140/RG.2.2.18470.55367.

Perea-Ardila, M.A., Oviedo-Barrero, F., Leal-Villamil, J.2019. Mangrove forest mapping through remote sensing imagery: study case for Buenaventura, Colombia. Revista de Teledetección,53, 73-86. <https://doi.org/10.4995/raet.2019.11684>

Hu, LuoJia & Xu, Nan & Liang, Jian & Li, Zhichao & Chen, Luzhen & Zhao, Feng. (2020). Advancing the Mapping of Mangrove Forests at National-Scale Using Sentinel-1 and Sentinel-2 Time-Series Data with Google Earth Engine: A Case Study in China. Remote Sensing. 10.3390/rs12193120.

Yancho, J.M.M.; Jones, T.G.; Gandhi, S.R.; Ferster, C.; Lin, A.; Glass, L. (2020) The Google Earth Engine Mangrove Mapping Methodology (GEEMMM). Remote Sens. 12, 3758. <https://doi.org/10.3390/rs12223758>

Supervisors of diploma thesis: **Mgr. Rostislav Nėtek, Ph.D.**  
**Department of Geoinformatics**

Date of assignment of diploma thesis: November 9, 2020

Submission deadline of diploma thesis: May 6, 2021

UNIVERZITA PALACKÉHO V OLOMOUCI  
PŘÍRODOVĚDECKÁ FAKULTA  
KATEDRA GEOINFORMATIKY  
17. listopadu 50, 771 46 Olomouc



L.S.

---

doc. RNDr. Martin Kubala, Ph.D.  
Dean

---

prof. RNDr. Vít Voženílek, CSc.  
Head of Department

# CONTENT

<b>INTRODUCTION .....</b>	<b>7</b>
<b>1 STATE OF THE ART .....</b>	<b>8</b>
<b>2 OBJECTIVES.....</b>	<b>11</b>
General objective .....	11
Specific objectives.....	11
Research questions.....	11
Thesis Structure.....	11
<b>3 OVERVIEW OF METHODS AND PROCEDURES.....</b>	<b>13</b>
3.1 Data .....	13
3.2 Methods .....	14
3.2.1 Classification methods .....	14
3.2.2 Visualization methods .....	15
3.3 Software .....	17
3.4 Processing procedure .....	18
<b>4 DATA AND SITE DESCRIPTION.....</b>	<b>19</b>
4.1 Input Data.....	19
4.1.1 Remote Sensing data.....	19
4.1.2 Reference maps and ancillary data .....	23
4.2 Site description.....	24
<b>5 MANGROVE COVER CLASSIFICATION.....</b>	<b>28</b>
5.1 Workflow description .....	28
5.2 Data pre-processing.....	29
5.2.1 Sentinel-2 pre-processing.....	29
5.2.2 Sentinel-1 pre-processing.....	37
5.3 Classification .....	41
5.3.1 Supervised classification .....	41
5.3.2 Training sites and validation data.....	43
5.3.3 Classification models.....	45
5.3.4 Temporal and spatial transferability .....	46
5.3.5 Validation and accuracy assessment .....	46
5.3.6 Results .....	47
<b>6 VISUALIZATION .....</b>	<b>54</b>
6.1 Geovisualization .....	54
6.2 Web mapping tools and libraries .....	55
6.3 Web map creation.....	57
6.3.1 User interface layout and input data.....	58
6.3.2 Data processing in ArcGIS Pro.....	59
6.3.3 Map styling in ArcGIS Online .....	60
6.3.4 Publishing the web map .....	61
6.4 Results .....	62

**7 DISCUSSION .....63**  
**8 CONCLUSION .....67**  
**REFERENCES**  
**ATTACHMENTS**



# INTRODUCTION

Mangrove forests are considered some of the most carbon-rich and productive ecosystems in the world and serve as an important factor in coastal protection. They grow in tropical or subtropical climates and are adapted to grow in intertidal areas where a combination of sea water and fresh river water are present, thanks to their salt tolerant roots. However, extreme climate events, and sea level rise, together with anthropogenic activities have been increasing the pressure on these important ecosystems, globally.

The development of effective methods for monitoring these ecosystems is crucial for assisting decision makers and managers protecting them and to help countries meet environmental targets (e.g Millennium Development Goals and Ramsar Convention on Wetlands of International Importance) (Kuenzer et al. 2011; UN Millenium Project, 2005; Ramsar Convention Secretariat, 2016). Remote sensing has proven to be essential in monitoring and mapping ecosystems and has been extensively applied to research and monitoring mangrove forest extent and dynamics (Zambrano and Rubiano 1996; Giri et al. 2011; Hamilton and Casey 2016; Shapiro et al. 2018; Bunting et al, 2018; Yancho et al.2020) but has commonly relied on coarse-to-medium scale resolution optical data. Most studies incorporate single optical satellite imagery for classification, Landsat satellites being most common, and a handful of studies have integrated Copernicus Sentinel-2 imagery with the Landsat for land cover classification (Chen et al. 2015; Tieng et al 2019). The production of mangrove cover products with higher resolution datasets like Sentinel-2 and combined with radar datasets, like Sentinel-1, can improve reliability of the results (Shapiro et al. 2018; Portengen, 2017; Borges et al. 2020). Moreover, methods for mangrove forest classification are often complex and not easily reproducible. Advancements in remote sensing technologies like the cloud-based Google Earth Engine platform, however, are making it more feasible to combine large amounts of multi-sensor earth observation data by reducing the need for high processing power, and to easily share the entire processes (Goldberg et al. 2020).

In Colombia, mangrove forests are located both in the coasts of the Caribbean and the Pacific region. According to Castellanos-Galindo et al. (2021), close to 80% of mangrove forests in the country are found along the pacific coastline. These mangroves are considered among the wettest in the world and are highly developed. A study carried by Simard et al., (2019), identified these forests as holding the tallest mangroves world-wide, together with the ones in Gabon, Africa. Being located in a humid tropical region poses a challenge for the extraction of accurate information with optical sensors, which are affected by cloud presence.

Considering the advantage that radar data, which is not affected by cloudy conditions, and free high-resolution optical data could bring to the table, this study investigates the potential benefits of using Sentinel-1 (radar) and Sentinel-2 (optical) imagery within the GEE environment to generate accurate estimations of mangrove forest extents, while summarizing a reproducible methodology. The derived classification model will be applied to the different departments of the region and the classification outputs will be integrated into a web map for easy access.

# 1 STATE OF THE ART

The following chapter describes the findings on the current knowledge of the studied topic according to the analysis of similar or related published work.

## **Importance of mangrove forest ecosystems so the Sustainable Development Goals (UN)**

Mangrove ecosystems are a valuable ecological and economic resource that represent some of the most carbon rich forests in the world. These ecosystems are nurturing and feeding grounds for many wildlife species and bring valuable ecological and economic benefits through their role in shoreline protection, sediment retention, climate change mitigation and water purification. Their importance is reflected in their role within multiple UN Sustainable Development Goals (SDG), from reducing poverty and hunger, to improving life below water and goals in between (Blum and Herr, 2017). Particularly, their protection and restoration directly addresses SDG 14, which focuses on sustainable governance our oceans and coasts and recognizes their great value to coastal communities, as well as SDG1 and SDG2 (eliminating poverty and hunger), SDG 8 (ensuring livelihoods and economic growth), SDG 13 (taking actions against climate change impacts) and SDG 15 (halting biodiversity loss) among others. Understanding and mapping the extent of mangrove ecosystems, is also particularly critical for the SDG 6, which is to “Ensure availability and sustainable management of water and sanitation for all”, addressed via the indicator 6.6.1 “Change in the extent of water-related ecosystems over time”. The observations generated from monitoring mangrove ecosystem extents and biomass, are therefore, essential for measuring our progress in meeting the SDG quotas (Blum and Herr, 2017)

## **Mapping mangrove forests in Colombia**

Colombia has consistently been listed as one of the top-20 mangrove-bearing countries worldwide, and one of the largest in the Western Hemisphere (Mejía-Rentería et al 2018). Approximately 70 to 80 percent of Colombia’s mangroves are located along the Pacific coast (Sánchez-Páez et al., 1997; Castellanos-Galindo et al., 2015), which are significantly preserved, especially compared to the relatively smaller and more impacted mangroves forests found along the country’s Caribbean coast (Blanco et al., 2012)

Within the Colombian territory, different institutions of the national and regional order have made efforts to determine preliminary environmental coastal zoning and their integrated management, including the cartography of mangrove forests, by implementing remote sensing and GIS techniques both along the Caribbean and Pacific coastline (Perea-Ardila et al., 2019; Zambrano and Rubiano, 1996; Blanco-Libreros, 2016). However, the country’s official land use and land cover (LULC) maps are not regularly updated, which constraints the information available to make informed decisions (Anaya et al., 2020).

According to Mejía-Rentería et al (2018), more mangrove studies have been made for the Caribbean coast compared to the Pacific coast, even though the Pacific coverage is far more substantial. The authors argue that this is likely influenced by the likelihood of reporting the more sizeable losses in the Caribbean, thereby increasing the chances of publishing significant results, as opposed to the Pacific Coast, where losses are expected to be less substantial. An additional factor, they propose, is that the infrastructure in the Caribbean coast is more developed and has better accessibility.

Throughout the literature review of this study, it was possible to find open-access datasets of global mangrove cover presented in the form of web maps, from where it is possible to download the datasets. Different examples of web maps containing or exclusively presenting mangrove cover data, found during this research and literature review, were for the most part produced at a global scale. The Global Mangrove Watch (GMW, 2018), for example, is a collaboration project between several institutions (Aberystwyth University, soloEO, UNEP-WCMC and JAXA) and is an online platform that provides remote sensing data and tools for mangrove monitoring. The GMW data portal gives access to near-real time extent and dynamics information of mangroves across the globe ([www.globalmangrovetwatch.org/](http://www.globalmangrovetwatch.org/)). Other examples are The Global Forest Watch ([www.globalforestwatch.org](http://www.globalforestwatch.org)) or the Global Mangrove Height and Biomass Explorer (Simard et al. 2019) ([mangrovescience.earthengine.app](http://mangrovescience.earthengine.app)), among others.

However, finding openly accessible Colombian mangrove dataset sources at regional or even national scale was challenging. It was also apparent, as Mejia et al. (2019) have revealed, that there have been more publications for mangroves on the Caribbean coast. As a result, this study relied primarily on the mangrove extent records published by other researchers and institutions (Mejía-Rentería et al. 2018; Orjuela, 2009; Invemar, 2010; Alvarez-León, 2018), and global mangrove datasets that were openly available. The following table shows the datasets used as reference for mangrove extents on the Colombian Pacific coast, as recorded by Mejía-Rentería et al. (2018)

**Table 1.** Historical mangrove area estimates on the Colombian Pacific coast. Adapted from Mejia et al (2018).

<b>Author(s)</b>	<b>Year(s)</b>	<b>Coverage/ spatial resolution</b>	<b>Methods and dataset accessibility</b>	<b>Pacific coast extent (ha)</b>
<b>IGAC (1966)</b>	1966		Re-interpreted map geo-referenced	360,000
<b>Zambrano- Escamilla and Rubiano- Rubiano (1996)</b>	1992	Colombia	STAR synthetic aperture radar (SAR) images taken in 1992 and traditional aerial photographs. <u>Access:</u> closed	292,724
<b>Mangrove Forests of the World (MWF) - Giri et al. 2011</b>	2000	Global/30m	Hybrid supervised/unsupervised classification (ISODATA y clustering). Landsat imagery <u>Access:</u> Open (Ocean Data Viewer/ GEE data catalogue)	151,752

<b>CGMFC-21— Hamilton and Casey (2016)</b>	2000- 2014	Global/30m	Masked Global Forest Change (GFC) maps using MFW) to calculate dynamics. Landsat imagery. <u>Access:</u> Open (2000–2012 data from CGMFC-21)	132,325
<b>Global Mangrove Watch (Bunting et al, 2018)</b>	1996, 2007– 2010, 2015– 2016	Global/25 m	Supervised classification (Random Forest); histogram thresholding. Jers-1, ALOS, ALOS-2, Landsat imagery <u>Access:</u> Open (Ocean Data Viewer and <a href="https://www.globalforestwatch.org/">https://www.globalforestwatch.org/</a> )	161,639
<b>SIGMA – INVEMAR, 2015 (2014)</b>	2014	Colombia	Compilation of different methods used by the regional environmental agencies.	209,402

The work by Mejia-Rentería et al. (2018) was a particularly valuable source of information as it provided a more recent reference of mangrove extents for each department of the pacific coast, to which to compare the results obtained from this study. The authors compared the historical values of mangrove extents reported for the Colombian Pacific coast and integrated new information produced since 2010 (Giri et al., 2011; Hamilton and Casey, 2016) in order to derive more accurate estimates for comparison at the departmental level. Estimates by Orjuela et al (2009) and Inveimar (2015) were included as additional national scale estimates for each department (Table 2).

**Table 2.** Mangrove cover extent estimates in Colombian Pacific coast, by department. Adapted from Mejia et al (2018) with added information.

<b>Province</b>	<b>IGAC (1966) 1966 (ha)</b>	<b>Zambrano- Escamilla and Rubiano- Rubiano (1996) (ha) 1992</b>	<b>Orjuela et al., 2009</b>	<b>Giri et al. (2011) 2000 (ha)</b>	<b>SIGMA (Inveimar, 2015) 2014 (ha)</b>	<b>Hamilton and Casey (2016) 2014 (ha)</b>	<b>GMW 2016 v2 (ha)</b>
<b>Chocó</b>	79,918.92	64,750.5	64,750	22,368.3	41,331.19	18,418.1	24,900
<b>Valle del Cauca</b>	48,396.42	41,961.4	31,374	30,155.9	31,478.06		20,288
<b>Cauca</b>	59,648.11	36,276.8	19,703	16,403.1	19,125.01	15,571.3	11,362
<b>Nariño</b>	172,083.65	149,735.8	117,576	76,382.2	117,468.57	76,262.0	105,089
<b>Total</b>	360,083.09	292,724.4	233,403	132,325.0	209,402.83	132,099.6	161,639

## **2 OBJECTIVES**

### **General objective**

The main objective of this thesis dissertation is to evaluate the combined use of optical and radar data following existing methodological approach to classify and delineate mangrove forest cover in the Colombian Pacific coast using the Sentinel-1 and Sentinel-2 mission products and Google Earth Engine, for the reduction of processing power requirements. Finally, to develop simple visualization products for presenting the results.

### **Specific objectives**

The specific objectives of this thesis dissertation will be to: (a) explore and process multi-sensor Earth Observation data to generate a spatially continuous mangrove forest cover map in an area of very high cloud cover persistence using the Copernicus Sentinel-1 and 2 imagery; (b) combine optical and radar data to evaluate whether classification accuracy is improved (c) explore transferability and reproducibility in other locations € present the results of the analysis the form of a web map.

To attain the objectives the following specific tasks will be carried out:

- Investigate, evaluate, and apply an existing mangrove forest cover mapping methodological approach.
- Classify mangrove forest cover from Sentinel-1 and Sentinel-2 satellite images by applying a machine-learning classification technique.
- Assess accuracy and validate results.
- Produce a web map application to visualize and access the classification outputs.

### **Research questions**

- 1. Does the combination of Sentinel-2 optical with Sentinel-1 radar data improve classification accuracies?**
- 2. Is the model transferable to other locations and years?**
- 3. What is an appropriate solution for visualizing the classification outputs?**

### **Thesis Structure**

The first chapter includes the definition of the objectives of the study, together with research questions. In the second chapter, general concepts and definitions of data methods and software used for the development of the study are presented. In the third

chapter an extensive literature review is included to provide a background on related studies and approaches that served as the baseline to develop the study. The fourth chapter discusses the methodology applied and is divided into two main parts, the classification methodological approach and the methods used for visualization of the resulting products. This chapter contains the approaches and steps that were followed to achieve the previously discussed goals, as well as constraints and limitations encountered. The fifth chapter summarizes the findings derived from the study both in terms of classification and visualization, together with a discussion of the advantages and disadvantages of the used methods. The final chapter covers concluding remarks and recommendations.

## **3 OVERVIEW OF METHODS AND PROCEDURES**

In this chapter, the methods, data and software used to comply with the objectives of the study will be briefly described. In the following chapters these methods and procedures will be analysed more extensively.

### **3.1 Data**

#### **Sentinel-1 satellite data**

Sentinel-1 is the first mission of Copernicus, the European Union's Earth Observation Program, and consists of a constellation of two identical radar satellites, Sentinel-1A (launched on April 2014) and Sentinel 1B (launched on April 2016), which are operated by the European Space Agency (ESA). Both satellites share the same orbital plane and carry a C-band Synthetic Aperture Radar (SAR) instrument which provides all-weather, day and night, imagery, and can offer reliable wide area monitoring. There is a wide range of applications for the data acquired via the Sentinel-1 mission, including land and sea monitoring and emergency response to environmental disasters, among others. The data is available for public, scientific, or commercial purposes and can be accessed directly through the Copernicus Open Access Hub ([scihub.copernicus.eu](http://scihub.copernicus.eu)) free of charge.

#### **Sentinel-2 satellite data**

Sentinel-2 is the second Copernicus earth observation mission consisting of two identical optical satellites, Sentinel-2A (launched in June 2015) and Sentinel-2B (launched in March 2017), also operated by ESA. Both satellites carry a multi-spectral imagery (MSI) with 13 spectral channels in the visible/near infrared (NIR) and short wave infrared spectral range (SWIR) with different resolutions. The Sentinel-2 mission data provides multispectral images designed primarily to monitor land cover and territorial change. The three bands in the red edge of the visible spectrum that the onboard sensor carries is especially suitable for examining the state of vegetation. It can be accessed directly through the Copernicus Open Access Hub ([scihub.copernicus.eu](http://scihub.copernicus.eu)) free of charge.

#### **Mangrove Forests of the World (MFW) (Giri et al., 2011)**

The MFW database was the first, most comprehensive mangrove assessment worldwide, and was developed by Giri et al., 2011. The database is based in Landsat satellite data from the year 2000. Over 1,000 scenes were classified using hybrid supervised and unsupervised classification techniques. The MFW serves as a baseline for mangrove monitoring, identifying priority areas for mangrove conservation, and studying the role of mangroves in coastal protection (e.g. tsunami), carbon sequestration and biodiversity (GEE Catalog, 2021). The database can be downloaded freely from the UNEP-WCMC webpage: <http://data.unep-wcmc.org/datasets/4>

#### **Global Mangrove Watch (GMW) 2016 mangrove dataset (Bunting et al. 2018)**

The Global Mangrove Watch (GMW) dataset is a global baseline map of mangroves generated from ALOS PALSAR and Landsat data for the year 2020, with the changes from this baseline for the period between 1996 and 2016, derived from JERS-1 SAR, ALOS PALSAR and ALOS-2 PALSAR-2. Each year (1996, 2007, 2008, 2009, 2010, 2015 and

2016) can be downloaded individually. and Overall, the GMW's objective is to provide organizations like the Ramsar Convention, and decision makers, mangrove extent and dynamics geospatial information. The dataset can be downloaded from: <https://data.unep-wcmc.org/datasets/45>

### **Global Mangrove Distribution, Aboveground Biomass, and Canopy Height (Simard et al., 2019)**

The dataset is based on remotely sensed data and in-situ field data and contains information on the global distribution, biomass and canopy height of mangrove forest wetlands. The data on above ground biomass (AGB), maximum canopy height (height of the tallest tree), and basal-area weighted height (tree heights in proportion of their basal area) were derived for the year 2000 over a 30-metre resolution global mangrove extent map. Extensive field in situ measurements were done to derive the final estimates and validate remotely sensed estimates. The dataset can be downloaded directly from: [https://daac.ornl.gov/cgi-bin/dsviewer.pl?ds\\_id=1665](https://daac.ornl.gov/cgi-bin/dsviewer.pl?ds_id=1665)

### **Continuous Mangrove Forest Cover for the 21st Century (CGMFC-21) (Hamilton and Casey, 2016)**

The CGMFC-21 is a raster dataset of mangrove forest cover and annual change from 2000 to 2012. The dataset has a 30-metre resolution within the tropics. The mangrove cover baseline is from the year 2000 (Giri et al. 2011) and the subsequent data is generated from Hansen et al. 2013). The data is reported by country and can be downloaded directly from the Harvard Dataverse: doi 10.13016/M2Q989.

### **ALOS Global Digital Surface Model "ALOS World 3D - 30m (AW3D30) - Elevation data**

The ALOSWorld3D 30m DSM v3.1 dataset provides a 30-metre resolution global surface model based in millions of images collected by the panchromatic optical sensor (PRISM) onboard the ADVANCED Land Observing Satellite (ALOS). The first version of the dataset was published in 2016 and has been updated to improve accuracies since then. The latest version which was used for the current study was released in April 2020, is freely available for all commercial and non-commercial purposes. The dataset is available in the Google Earth Engine repository and has been widely used in scientific research with solid accuracy (UUemaa et al. 2020; Courty et al. 2019; Jain et al 2018). Alternatively, the data can be downloaded from:

<https://www.eorc.jaxa.jp/ALOS/en/aw3d30/index.htm>

## **3.2 Methods**

### **3.2.1 Classification methods**

#### **Google Earth Engine Mangrove Mapping Methodology (GEEMMW)**

GEEMMM is a freely accessible tool for mapping and monitoring mangrove ecosystems worldwide. It was designed by Yancho et al, (2020) to provide a ready-to-use methodology for non-experts, and thus runs on detailed and well-commented code within the GEE



environment. Users need a basic understanding of the key steps required for mapping mangroves, as well as basic computer skills. The interactive tool is broken into three modules – Module 1: Region of interest definition and Landsat composite generation; Module 2: spectral separation examination, multi-date classification and accuracy assessment; Module 3: dynamics exploration and optional QAA.

### **Pixel-based Supervised classification**

Supervised classification is a commonly used procedure for quantitatively analysing remote sensing derived data. This method requires reference samples of specific classes to train the classifier and class the unknown data. Thus, by selecting representative sample sites, the user specifies the pixels or spectral signatures that will be associated to each class and can classify the entire image, generating a land cover map (Richards, 1986).

### **Random Forest classifier**

Random Forest is an ensemble classifier that generates multiple decision trees applying a randomly selected subset of training samples based on the dataset attributes of interest. It is a supervised algorithm which seeks to improve prediction power by combining the outcomes of different iterations of the same algorithm. Finally, the chosen prediction for the pixels will correspond to the most voted class among all the decision trees (Belgiu and Dragut, 2016).

## **3.2.2 Visualization methods**

### **Geovisualization**

Geovisualization, which is short for “Geographic Visualization“, can be defined as a modern form of cartography in which the map is not only a representation, but rather a model for geospatial-oriented scientific visualization (Huisman & de By, 2009). It refers to tools and methods that support spatial data analysis and communication, and therefore are crucial for data exploration and decision-making processes. Geovisualization integrates approaches from visualization in scientific computing, cartography, image analysis, information visualization, exploratory data analysis, and geographic information systems among others, to provide theory, methods and tools for visual exploration, analysis, synthesis, and presentation of geospatial data (MacEachren and Kraak, 2001).

### **Web Map**

A web map is a map that is displayed via the internet and can be static or dynamic. A web map can be accessed as long as there is an internet connection from any device with an internet browser (Dorman, 2020). Examples of web maps are Google Maps or OpenStreetMap.

### **User interface (UI)**

User interface is a set of elements on the page that the user can see and/or manipulate. (Sack, 2017). In other words, it is the space where interactions between humans and

machines take place. The objective of this interaction is to allow the most effective operation and control of the machine from the interaction with the user

### **HTML and CSS**

HTML (Hypertext Markup Language) and CSS (Cascading Style Sheets) are two core technologies for building websites. They are the basis of website and web application building. HTML provides the structure of the content, by designing the function of each element in a page, while CSS provides the aesthetics of the layout, defining colour, sizes, font, element positions, etc.

### **JavaScript**

JavaScript (Brendan Eich, 1995) is a scripting programming language for implementing functions into websites. JavaScript is used by most pages that contain dynamically updated content, interactive features, including interactive maps, animated 2D and 3D graphics, video players, and similar features. JavaScript was standardized 1998 by ISO (International Organization for Standardization) and runs on the client side. However, there are also implementations for the server-side. With its functionality, it complements the core web technologies: HTML and CSS.

### **Tiff, GeoTiff (raster format)**

Tiff (Tag Image File Format) is a frequently used format for storing raster spatial data. It's geoTIFF variant is more commonly used in the field of geoinformatics, which contains information about the file's coordinate system in the header. Aerial survey images are an example of data commonly stored in the GeoTIFF format.

### **GeoJson**

GeoJSON is an interoperable geospatial format based on the JSON (Java Script Object Notation) data format, which is a universal format that can be processed in any programming language. With the exception of ESRI's ArcGIS desktop, the format is supported by all major GIS software. GeoJSON defines several types of JSON objects and their combination to represent geographic features, their properties and spatial scope. The data can be stored in point, line, polygon, multipoint, multiline, multipolygon or a collection of geometries. The format is platform independent and has a simple structure. GeoJSON uses the WGS84 (World Geodetic System 1984) coordinate system and decimal degrees (Nétek et al.,2019).

### **Raster tile**

A raster tile is the basic data unit for transferring raster data over a network. Tiles are used to divide a raster into small manageable pieces. One of the benefits of subdividing a raster into tiles is to improve performance.

### **Shapefile**

Shapefile was originally an Esri proprietary format, that was later adopted as a standard format. The format was developed in the 1990s when web solutions did not yet exist and is not suitable for use in data transfer on the web. It is supported by almost all geographic information systems (GIS) and is always stored in 3–6 files (\*.shp, \*.shx, \*.dbf, \*.prj,...).

## **Generalization**

Map generalization, or simply generalization, is a process related to the application of a set of algorithms to geographic data, in order to control the optimal representation of geospatial phenomena at a range of scales or levels of detail.

## **3.3 Software**

### **Google Earth Engine**

Google Earth Engine (GEE) (Gorelick et al. 2017) is a cloud-based computing platform established to support planetary-scale geospatial data analysis, processing, and visualization. GEE is free for non-commercial use and has an easy account creation process. GEE provides access to a petabyte-scale archive of publicly available remotely sensed imagery, ancillary data, and computational tools to achieve a wide range of remote sensing and geospatial tasks at very high speeds and scales. Since it was released in 2010 it has developed steadily and is now a well-established tool for large-scale geospatial analysis.

### **ArcGIS Pro**

ArcGIS Pro is a desktop GIS application for creating and working with spatial data. It provides tools for visualization, analysis, compilation, and sharing data in 2D and 3D settings. ArcGIS Pro is a 64-bit application, which is part of ArcGIS Desktop. However, it is an application connected to the web and integrated with ArcGIS online.

### **ArcGIS Online**

Esri's ArcGIS Online is a cloud-based analysis and mapping platform developed by ESRI. Esri established ArcGIS online in 2007 for the creation, analysis and use of maps integrating several functions from the Esri ArcGIS desktop software.

### **ESRI Web AppBuilder**

Web AppBuilder is a tool provided by ESRI to create web mapping applications in a simple and intuitive way. It uses HTML5 and JavaScript and can be found as part of the ArcGIS Online, the Portal for ArcGIS, or as a standalone version of Developer. The Developer edition provides an extensible framework allowing the customization of widgets and themes.

### **MapTiler**

MapTiler is a software developed to subdivide raster images to tiles and publish them on the web. The Czech-developed software is a successor to the GDAL2Tiles software and can be used as a desktop application as well as on the cloud. The output allows you to get tiles in a folder structure, in MBTiles or GeoPackage format. There are two cloud platforms to choose from: MapTiler Cloud or Google Cloud Storage. Since the version release at the end of 2018, it processes vector data in addition to the raster data.

### 3.4 Processing procedure

The Pacific coast mangrove extent was mapped primarily based on the workflow and semi-automated mangrove mapping methods applied by Shapiro et al. (2018). The analysis structure and methods were further supported and adapted according to approaches applied by Yancho et al. (2020) within the Google Earth Engine Mangrove Mapping Methodology. The mangrove cover extent was obtained by applying a pixel-based supervised classification approach and a Random Forest classifier. The data used for the classification were composites derived from a combination of Sentinel-1 and Sentinel-2 images and a set of indices. Finally, the results are presented in the form of simple web map products for easy access. The general processing workflow is shown in Figure 1.

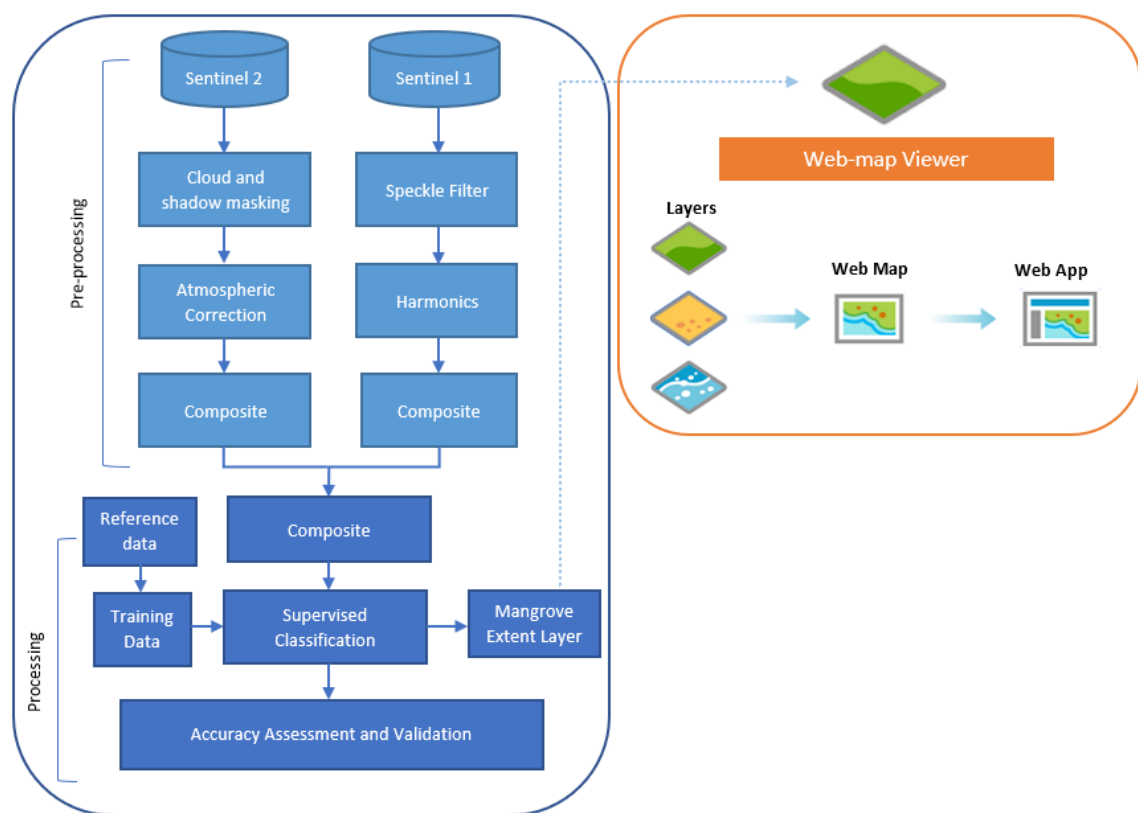


**Fig 1.** Processing workflow

## **4 DATA AND SITE DESCRIPTION**

Chapter three provides an overview of the data used for implementing the study. In this chapter, a more thorough description of the data will be given, especially in regard to the Sentinel-1 and Sentinel-2 data. Technical specifications and settings used in for the study will be included in this chapter. The study area will also be described to provide the reader a general idea of the context in which the study was developed.

### **4.1 Input Data**

#### **4.1.1 Remote Sensing data**

The data used for any land cover classification scheme has a significant impact on the research outcomes. The environmental domain especially benefits from increased spatial and temporal resolution. However, it is important to consider not only the technical specifications but also the availability if free accessible data.

Copernicus is the European Union's (EU) Earth observation program. The program has a free, full, and open data access policy that provides access to millions of scenes with higher temporal and spatial resolution to anyone interested. At present it operates 7 missions under the Sentinel program (Sentinel missions 1, 2, 3, 4, 5p, 5, 6), which can be accessed directly through the Copernicus Open Access Hub ([scihub.copernicus.eu](https://scihub.copernicus.eu)), as well as through other platforms such as Google Earth Engine (GEE) (Gorelick et al. 2017) and Amazon Web Services (Amazon 2016).

GEE offers an extensive data catalogue that is constantly updated and includes data from the seven currently operating Copernicus Sentinel missions. Furthermore, GEE is extremely helpful at applying aggregation of data to fill in major gaps due to cloud cover, avoiding the need to download large amounts of data and process each image for integration before conducting the actual analysis (Kumar and Mutanga. 2019). Thus, for the scope of this study, the entire classification process was performed within the GEE cloud-based platform. Images from the Sentinel-1 GRD and Sentinel-2 Level-1C products were accessed from GEE's repository and processed directly in the code editor of GEE's JavaScript API.

#### **Sentinel-1**

The Copernicus Sentinel-1 mission is primarily used for monitoring land, sea, ocean, coasts, ice, and polar regions. Some specific applications include crop monitoring, soil moisture measuring, wetland monitoring, biomass estimation, ship detection, oil spill detection etc.

The Sentinel-1 (S1) mission is a constellation of two satellites (Sentinel-1A and Sentinel-1B). The constellation orbits  $180^\circ \pm$  apart, which means that the mission images Europe every six days and the rest of the world every twelve days. It operates day and night,

regardless of illumination and weather conditions, collecting imagery via its C-band Synthetic Aperture Radar (SAR) instrument. The SAR, which is made of antennas of a wavelength between 3,75 to 7,5 cm (4.0 to 8.0 gigahertz (GHz)) (figure 2), collects imagery at different instrument configurations, band combinations and resolutions. Sentinel-1 can operate in four radar modes: Interferometric Wide Swath (IW), Extra Wide Swath (EW), Wave (WV) and Strip map (SM), and these modes can operate in several polarization schemes. The Sentinel-1 SAR system is a phase-preserving dual polarization system, which can transmit signals either in horizontal (H) or vertical (V) polarizations and receive in both (H and V). By varying the polarization of the transmitted signal, SAR systems provide information on the polarimetric properties of the observed surface (GEE, 2020).

1. transmitterReceiverPolarisation: ['VV'], ['HH'], ['VV', 'VH'], or ['HH', 'HV']
2. instrumentMode: 'IW' (Interferometric Wide Swath), 'EW' (Extra Wide Swath) or 'SM' (Strip Map).
3. orbitProperties\_pass: 'ASCENDING' or 'DESCENDING'
4. resolution\_meters: 10, 25 or 40
5. resolution: 'M' (medium) or 'H' (high).

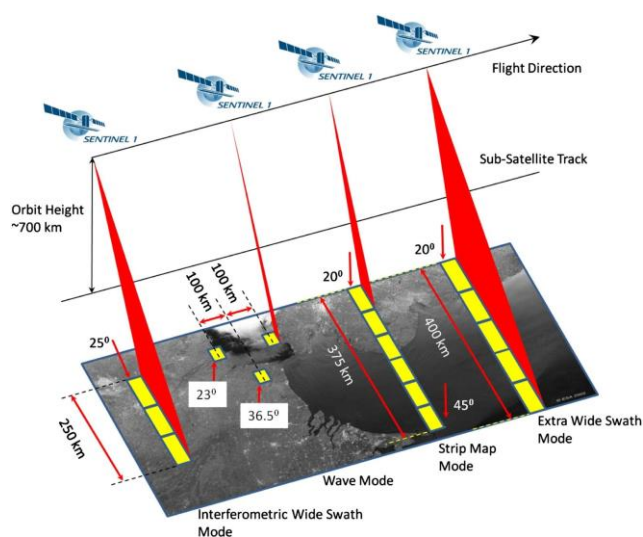


**Fig 2.** Sentinel-1 Product modes. Source: ESA (sentinel.esa.int)

The Sentinel-1 Level-1 data are distributed under two product types by the Copernicus Open Access Hub, Single Look Complex (SLC) and Ground Range Detected (GRD). The Sentinel-1 collection that is available in the GEE catalogue corresponds to Level-1 Ground Range Detected (GRD) scenes, which has been pre-processed from Level-1 Single Look Complex (SLC). This product consists of focused SAR data that has been detected, multi-looked and projected to ground range.

The data is continuously ingested by the GEE repository within two days after they become available. The scenes can be found in 10, 25 or 40m resolution and in three different instrument modes: IW, EW, SM. The radar in IW mode, used in this study, acquires data at 5m X 20m spatial resolution with 250km swath. Depending on the instrument polarization settings they will contain one or two polarization bands, out of

the four possible bands. Either a single VV or HH band and dual VV+HH or HH+VV band are possible. (GEE, 2020).

**Table 3.** Sentinel-1 polarization bands

VV	single co-polarization, vertical transmit/vertical receive
HH	single co-polarization, horizontal transmit/horizontal receive
VV + VH	dual-band cross-polarization, vertical transmit/horizontal receive
HH + HV	dual-band cross-polarization, horizontal transmit/vertical receive

For the present study, the collection was filtered to acquire all images at 10m resolution, Interferometric (IW) and both VV and VH polarizations, based on the workflows in Shapiro et al. (2018) and Portengen (2017). The pre-processed GRD data has been calibrated and orthorectified using the Sentinel-1 Toolbox. This process involves thermal noise removal, radiometric calibration, and terrain correction (using STRM 30m) of the images. Finally, the final terrain-correlated values are converted to decibels (dB), clipped to the 1<sup>st</sup> and 99<sup>th</sup> percentiles (to preserve the range against anomalous outliers), and quantized to 16 bits (GEE, 2020)

### **Sentinel-2 imagery**

The Copernicus Sentinel-2 mission provides multispectral images designed for monitoring land, as well as ocean and marine ecosystems. It also feeds data to services for applications in the Copernicus areas of emergency management and security. Some applications include LULC, territorial dynamics, vegetation state, forest management, water management, agriculture, ocean dynamics, natural disasters, and border surveillance.

The mission is composed of two satellites, Sentinel-2A, which was launched on the 23rd of June 2015, and Sentinel-2B, which was launched on the 7th of March 2017. However, the Sentinel-2A data did not become available until January 2016, and the data from Sentinel-2B until September 2017. Up until October 2019 the revisit time of both satellites varied considerably depending on the location of the globe, taking 5 days for Europe, Africa and Greenland (plus some other locations), and 10 days for the rest of the world. However, presently the satellites together have a 5-day revisit frequency for most parts of the world (ESA).

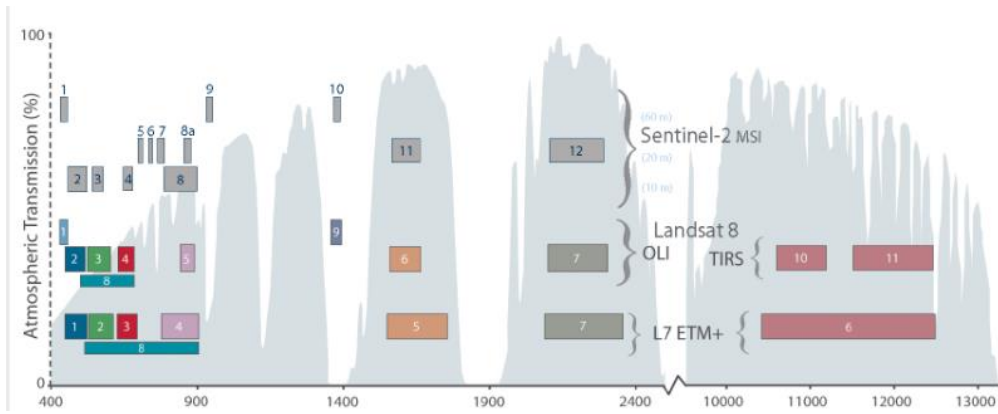


**Fig. 3** Spectral bands of Sentinel-2. Source: ESA (<https://sentinels.copernicus.eu>)

The Sentinel-2 MSI covers thirteen spectral bands (443–2190 nm), with a swath width of 290 km and a spatial resolution of 10m, 20m and 60m, depending on the spectral band. The four visible and near infrared bands at 10m resolution ensure the continuity with missions like Landsat-8 and SPOT-5 and address the user requirements particularly for land-cover classification. The six 20m red-edge and shortwave infrared bands meet the requirements for enhanced land-cover classification and geophysical parameter retrieval. Finally, the three 60m bands are dedicated mainly to atmospheric corrections. Wavelength and resolution specifications are found in Table 4. The bands used in this study were B2 (blue), B3 (green), B4 (red), B5 (vegetation red edge), B6 (vegetation red edge), B8 (near infra-red) and B8a (vegetation red edge).

**Table 4** Spectral bands for Sentinel-2B sensors

Sentinel-2 Bands	Central wavelength (nm)	Spatial resolution (m)
Band 1 – Coastal aerosol	442.2	60
Band 2 – Blue	492.1	10
Band 3 – Green	559.0	10
Band 4 – Red	664.9	10
Band 5 – Vegetation red edge	703.8	20
Band 6 – Vegetation red edge	739.1	20
Band 7 – Vegetation red edge	779.7	20
Band 8 – NIR	832.9	10
Band 8A – Narrow NIR	864.0	20
Band 9 – Water vapour	943.2	60
Band 10 – SWIR – Cirrus	1376.9	60
Band 11 – SWIR	1610.4	20
Band 12 – SWIR	2185.7	20

The S2 satellites undertake systematic acquisitions in a single observation mode, and the data is available at different levels (see Table 5). Level-1C (L1C) and Level 2A (L2A) are available in the GEE repository. L1C was the product used for the present study.



**Table 5** Sentinel-2 levels of data

<b>Level 1</b>	Top of atmosphere radiances (TOA)
Level-1B	Sensor geometry
Level-1C	Fixed cartography geometry (UTM projection and WGS84 ellipsoid)
<b>Level 2A</b>	Bottom of Atmosphere (BOA) reflectance in cartographic geometry

#### 4.1.2 Reference maps and ancillary data

Integration of supporting data such as known mangrove maps, elevation data and proximity variables (e.g. proximity from coastline) can help improve the accuracy of mangrove classification results, compared to using satellite imagery only (Liu et al. 2008; Shapiro et al; 2015; Shapiro et al, 2018; Yancho et al., 2020). Existing mangrove maps and recorded extent values were not only useful to compare outputs but were used to delimit the classification area (e.g. using a buffer from a known mangrove dataset) during the classification and post-classification process. The classification process was further supported by setting elevation thresholds and distances from the coastline. Altogether supporting data was used to reduce the chances of overestimation and improve the accuracy of the classification. Table 6 identifies the data that was used to support the satellite imagery in the classification of mangrove forests in the Colombian Pacific coast.

**Table 6.** Ancillary data used during the classification process.

<b>Ancillary data</b>				
<b>Name</b>	<b>Description</b>	<b>Use</b>	<b>Format</b>	<b>Source</b>
MFV 2010 (Giri, et al. 2011)	Global mangrove cover database derived from Landsat	Reference – ROI delimitation & visual validation	GeoTIFF	GEE catalog - <a href="https://developers.google.com/earth-engine/datasets">https://developers.google.com/earth-engine/datasets</a>
GMW 2016	The Global Mangrove Watch (1996-2016) dataset.	Reference – quantitative validation assessment	GeoJSON/ SHP	UN WCMC database <a href="https://data.unep-wcmc.org/datasets/45">https://data.unep-wcmc.org/datasets/45</a>
Hmax 95 Simard et al. (2019)	Global distribution and canopy height of mangrove-forested wetlands	Mangrove reference – post-classification	GeoTiff	Oak Ridge National Laboratory (ORNL) Distributed Active Archive Center (DAAC): <a href="https://daac.ornl.gov/cgi-bin/dsviewer.pl?ds_id=1665">https://daac.ornl.gov/cgi-bin/dsviewer.pl?ds_id=1665</a>
Mangrove distribution map (SIGMA)	Mangrove distribution map from the information System for the management of	Reference - visual validation	Web map (visual validation)	Invemar web map application - <a href="http://sigma.invemar.org.co/geovisor">http://sigma.invemar.org.co/geovisor</a>

	Colombian mangroves (SIGMA)			
MERIT DEM (Yamazaki et al. 2017)	Multi-Error-Removed Improved-Terrain (MERIT) DEM. High accuracy global DEM at 3 arc second resolution (~90 m at the equator)	Elevation data – Classification area delimitation (data-stack masking)	GeoTIFF	GEE catalog - <a href="https://developers.google.com/earth-engine/datasets">https://developers.google.com/earth-engine/datasets</a>
Admin Colombia	Level 0 (country) and Level-1 (departments) administrative boundaries	Coastline – proximity variable for ROI delimitation & Administrative boarders layer for web-map	Shapefile	Esri Colombia open data - <a href="https://datosabiertos.esri.co/">https://datosabiertos.esri.co/</a>
Drone Images	Acquired in 2019 by ....	Visual qualitative validation	GeoTiff	Field work images collected and shared by Gustavo Castellanos-Galindo

## 4.2 Site description

Colombia has approximately 1300 km of coastline along the Pacific Coast, which is shared by the departments of Chocó, Valle del Cauca, Cauca and Nariño. The southern 800km are dominated by low alluvial plains where many rivers that originate from the Andean Western Cordillera drain into the ocean. Compared to the national average of 33 people per km<sup>2</sup>, the Colombian Pacific coast population is considerably low, with only 5 to 17 people per km<sup>2</sup> (Etter et al., 2006).

The Colombian Pacific coast is highly biodiverse thanks to its coral ecosystems, mangrove forests, coastal lagoons, estuaries, beaches, and cliffs (Invemar, 2014). The mangrove forest ecosystem occupies approximately 232,391 ha of its land, with the largest extension in the department of Nariño (117,576 ha) (Orjuela et al., 2009).

Traditionally, mangroves have been harvested for fuelwood and as construction material. Poor planning and management of these activities have resulted in their overexploitation and deterioration, which has impacted on the socioeconomic well-being of the local communities that depend on them (Alvarez-León, 2019). Today, forest degradation constitutes an increasing pressure for conservation of biodiversity in coastal and protected areas of the region (Clerici, 2020).

According to a report by Invemar (2015), the Pacific Coast contains 209,402 ha of mangrove forests. They extend almost continuously from the Mataje River (south of

Nariño) to Cape Corrientes (Chocó department). Smaller patches are also found along the Tribugá Gulf and the inlets of Utría and Juradó (Choco department) near the border with Panamá (Vasquez, 2019). The high productivity of these ecosystems and their importance for sustaining the livelihoods of fishing and forestry communities has helped support Colombia's economic development (Alvarez-León, 2019).

The Pacific coast mangroves forests consist of both developed and young growth individuals, supporting a high diversity of true mangrove as well as associate species. There are eight mangrove-exclusive species in Colombia and all eight are found along the Pacific coastline, while five are found along the Caribbean coast. These include, *Avicennia germinans*, *Conocarpus erecta*, *Laguncularia racemosa*, *Mora oleifera*, *Pellicera rhizophorae*, *Rhizophora harrisoni*, *Rhizophora mangle* and *Rhizophora racemosa*. *Rhizophora* forests are more commonly found at the seafront, while *Avicennia-Laguncularia* forests are rather a dominant tidal forest type, but often found mixed with other mangrove species like *Conocarpus* or *Pelliciera*. The transition into land forest is represented by dry land mangroves, which are found towards the landward side of the core mangrove areas. This last group is only occasionally inundated and is often more diverse (Alvarez-León, 2019).

Due to the extent of the coastline and elevated processing time that it would require to run each process in such a large area, a smaller section of the coastline was selected for initially testing the classification models, and performing the adjustment and assessment of results. Considering the location and size, the selected pilot region was the Cauca department (Figure 3). The derived classification model was later applied to all departments of the Colombian Pacific coast to determine the full extent of mangroves along the pacific and at the same time evaluate the transferability of the model.



**Fig. 3** Location of the study’s region of interest and the four provinces (Chocó, Valle del Cauca, Cauca and Nariño).

### **Atmospheric conditions**

The Colombian Pacific coast is considered to be one of the regions with the largest annual precipitation globally and is characterized by persistent cloud cover (Simard et al 2019; Wilson and Jetz, 2016). It presents an absent or short dry season, with precipitation values found in large part of the coastline of over 5000mm/year (Correa and Morton, 2010). The CHIRPS database (Funk et al 2021) available in the GEE repository was processed to obtain the rainfall for the year 2020 in the region of interest, and to validate the afore recorded precipitation values. According to the CHIRPS dataset, filtered for the year and region of interest, the average total yearly rainfall was 4213 mm for the entire Colombian Pacific coast (defined as the area covering 20km inwards from the coastline). The Cauca department coastal area presented a 2020 average total of 4891 mm.

These conditions explain the heavy cloud persistence that characterizes the study area. Wilson and Jetz (2016), in their findings demonstrated that the tropical and subtropical biomes have the highest mean annual frequency and extremely low intra-annual variability, globally. The Colombian Pacific coast, according to their study, presents a mean annual cloud frequency that is close to one hundred percent, due to the low

seasonality and interannual variability of cloud presence in the area (Figure 5) (Wilson and Jetz, 2016). Therefore, the study ROI is clearly a hotspot of cloud stability, and consequently, detecting, and distinguishing land cover types can become a challenging task (Figure 5).

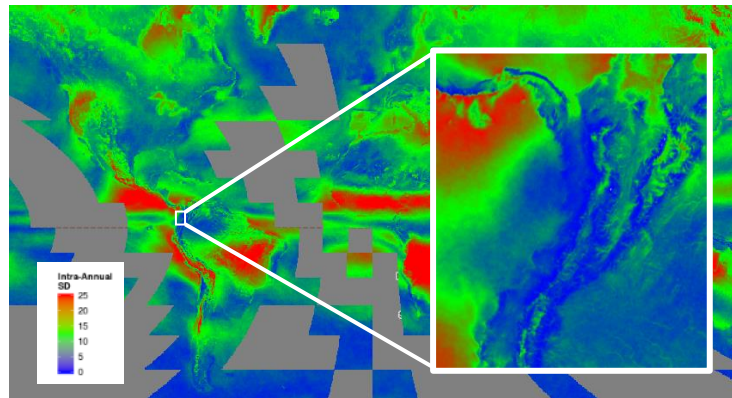


**Fig 5.** Distribution of seasonal cloud concentration in Colombia and globally, adapted from Wilson and Jetz, (2016). The intra-annual variation is defined as the standard deviation of the 12 monthly mean cloud frequencies, where red indicates areas with most variability and dark blue with no significant variability.

## 5 MANGROVE COVER CLASSIFICATION

The followed procedures and parameters used for classifying mangrove cover are explained in detail in this chapter. For this study, due to the atmospheric conditions of the region, the optical-radar fusion approach was chosen and applied with Sentinel-1 and Sentinel-2 imagery. After the filtering steps were applied, the optical and radar mosaics were built and stacked together with the pre-processed indices. Subsequently, a land cover classification and validation were performed through the implementation of a random forest algorithm, all within the GEE platform. The link to the GEE repository containing the scripts developed in the study can be found in Appendix I.

### 5.1 Workflow description

All processing of imagery and subsequent mangrove classification were performed in Google Earth Engine. Through an exploratory data analysis, the information that can be extracted from the Sentinel-1 and 2 satellite imagery was evaluated. The methods used for classifying mangrove cover extent along the Colombian Pacific coast were based primarily on the semi-automated mangrove cover classification workflow developed by Shapiro et al. (2018) and Yancho et al. (2020) (Google Earth Engine Mangrove Mapping Methodology). The adapted procedures were integrated and applied to the Colombian Pacific coast, using Sentinel 1 and Sentinel 2 imagery. A pixel-based supervised classification (using a Random Forest classifier) was performed to obtain the results for the department of Cauca, Colombia. The process (figure 6) was finally applied to the rest of departments of the Colombian Pacific (Chocó, Valle del Cauca and Nariño), in order to test transferability.

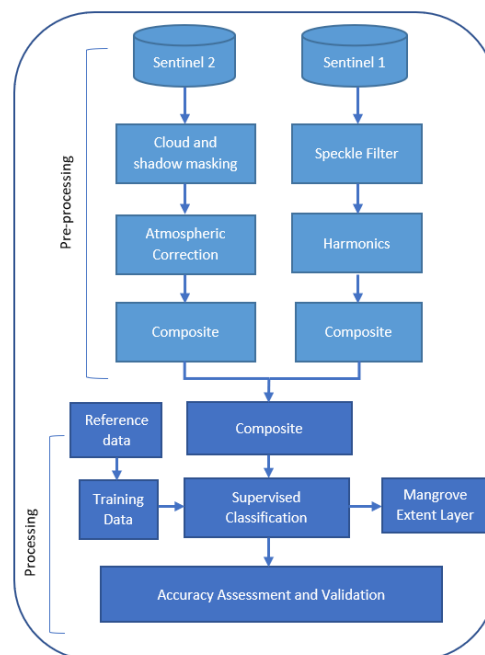


**Fig 6.** Processing workflow

## 5.2 Data pre-processing

The pre-processing workflow for the Copernicus Sentinel-1 GRD and Sentinel-2 L1C data is presented in the following sections. It was based primarily on the workflow applied by Shapiro et al. 2018, including the scripts developed for their research, and is further supported by the workflow and scripts of Yancho et al., (2020). Adjustments and some additions were made to adapt the scripts to this study, which will be highlighted.

All pre-processing was performed in the Google Earth Engine (GEE) cloud environment. This involved the preparation of cloud-free S2 and filtered S1 composites using all available images that fell under the defined conditions over the period of a year (2020). The resulting composites were then used to derive several spectral indices (NDVI, NDMI, MVI, etc) and all the bands of both datasets were stacked together to make the image used for classification. The steps are explained in detail in the following sections.

### 5.2.1 Sentinel-2 pre-processing

#### Defining the final ROI

The first step was to define the region of interest (ROI) boundaries that would be used to generate yearly Sentinel-1 and Sentinel-2 composites. Using the drawing tool in the GEE map a preliminary ROI was defined which was later used to clip the rest of the user-defined datasets needed to derive the final ROI. For the study, the Cauca department was chosen as the sample area to develop and test the classification workflow derived from a combination of Shapiro et al. (2018) and Yancho et al. (2020).

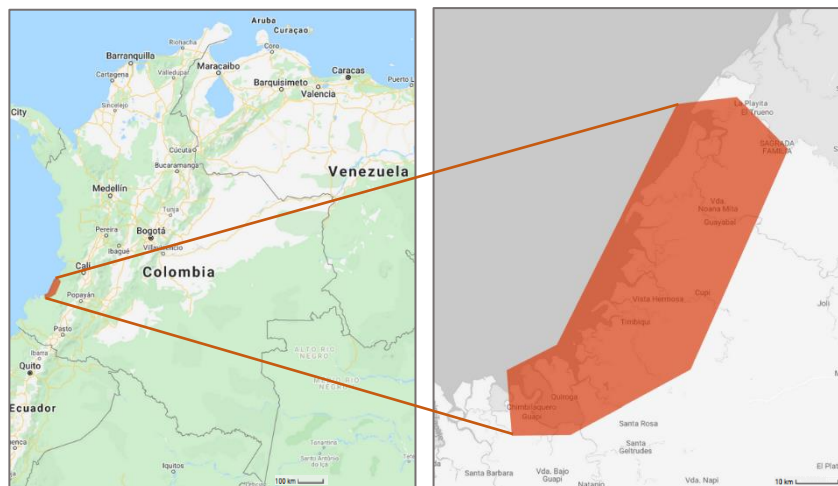


**Fig 6.** Manually defined preliminary ROI (Google basemap)

The known mangrove distribution layer, in this case the Global Mangrove Forest dataset from Giri et al. (2011), and a coastline layer (extracted from the administrative boarder dataset), were used to define the final ROI, following the approach applied by Yancho et

al. (2020). The aim is to make sure that the known mangrove dataset falls within the preliminary ROI, by including a buffer from the edge of that dataset. This approach has been demonstrated by different studies (Yancho et al. 2020; Giri et al 2011; Jones et al 2016) and helps overestimations on unnecessary scene areas. Finally, for the study area, the suggested minimum ROI extended 10km from the coastline (Fig 7).

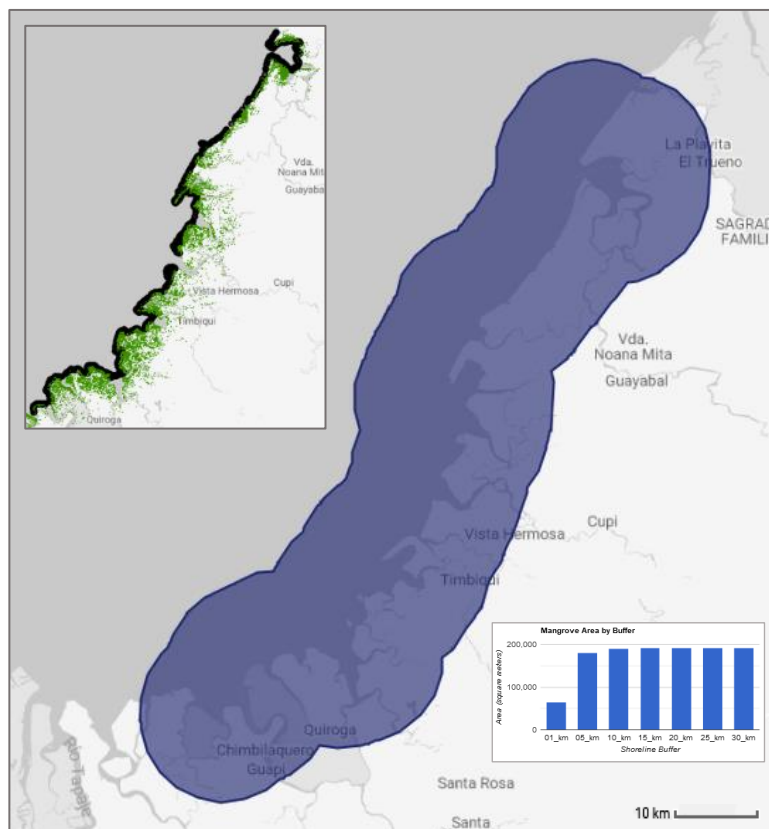


**Fig 7.** Final ROI (Google basemap)

### Data filtering

The next step was to determine the criteria for the Sentinel-2 image collection that would be used to obtain the composite used for the classification. The first question was to determine whether the Sentinel-2 L2A SR (surface reflectance) or the Sentinel-2 L1C TOA (top of atmosphere) product would be used.

The L1C data requires atmospheric correction, which can be done using the Sen2Cor processor in SNAP (Sentinel Application Platform). Sen2cor converts L1C to L2A products and includes not only atmospheric correction to bottom of atmosphere reflectance, but scene classification as well. Alternatively, both Sentinel-2 L1C and L2A data can be accessed directly through the Google Earth Engine catalogue and imported into the code editor for processing directly in the cloud.

The L2A product, has been used in many studies as it is corrected to surface reflectance and, from a theoretical point of view, should provide better results and less processing time. However, L2A data has not been produced for all L1C assets and depending on the



area of interest it is possible to encounter insufficient availability of Level 2A data. The GEE repository Sentinel-2 ingestion status was investigated, to obtain the coverage of the GEE repository TOA and SR products in the study area. The data availability can be seen in the graph below (figure 8).

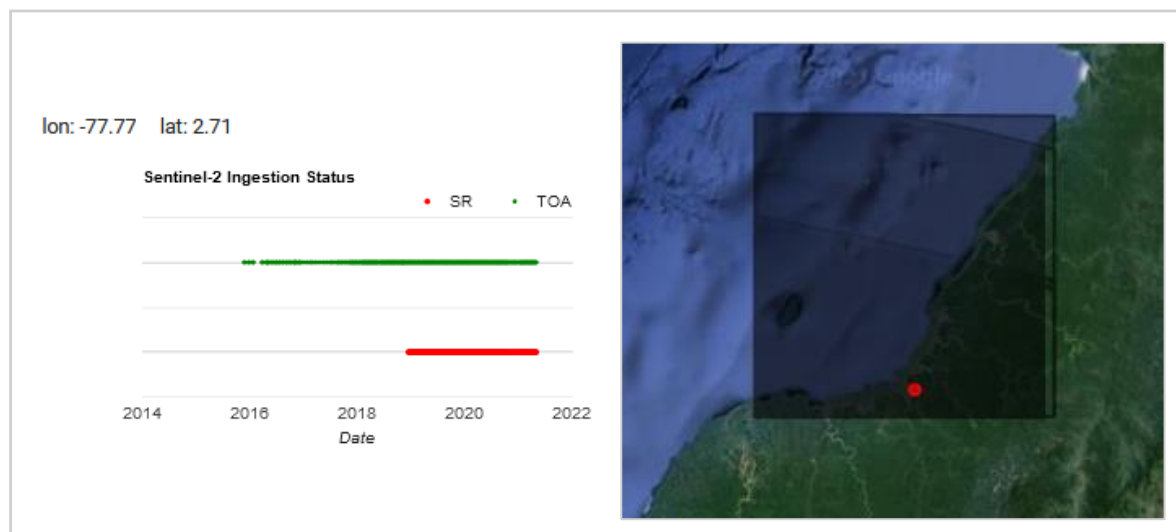


**Fig 8.** Sentinel-2 image ingestion status for the ROI (Google basemap)

The L2A product data at present is only partially available within a limited geographical and temporal range (Sudmanns et al. 2020). Not L1C imagery has been processed to L2A images by ESA, and therefore the L2A product has a reduced coverage within the GEE repository, that feeds on ESA's processed products. Consequently, the L1C product covers a wider time range for the region of interest than the L2A product. Although the preliminary study is done for the year 2020 initially, which is quite well covered by L2A images for the study area, the number of images is still larger in the L1C product. Also, the possibility of applying the classification algorithm at different spatio-temporal ranges was of interest to increase the potential repeatability, transferability, and scalability of the study. The Sentinel-2 Level-1C TOA reflectance data product in the GEE (ImageCollection ID: COPERNICUS/S2) was hence selected for the classification.

All Sentinel-2 images that intersected the study area between 1 January 2020 and 31 December 2020, with less than 75% cloud cover (Borges et al. 2020) were collected. The choice of setting a high cloud cover limit was made in order not to limit the number of images available, and preserve even the smallest cloud-free patches present in images. Setting a high limit meant that most images that could possibly have cloud free pixels were kept. All the bands were then resampled to 10m resolution (Shapiro et al. 2015; Shapiro et al 2018) and the next step was to mask clouds and shadow to derive the cloud free composites.

### **Atmospheric correction and cloud removal**

Cloud presence is one of the biggest concerns in spaceborne optical remote sensing, because it hampers a continuous monitoring of the Earth's surface (Schmitt et al., 2019).

Cloud, cirrus and shadow detection is not easy to attain, and consequently, dealing with cloud cover was one of the most demanding tasks of this study.

A drawback of selecting the Sentinel-2 L1C product is that it has to be atmospherically corrected and therefore, requires more processing time. This step involved removing clouds and shadow from the images in order to produce suitable composites for the classification to be reliable. One way to perform the L1C data atmospheric correction, is using the Sen2Cor processor in SNAP (Sentinel Application Platform). Sen2Cor converts Level 1C to Level-2A products and includes not only atmospheric correction to bottom of atmosphere reflectance, but scene classification as well. Alternatively, Sentinel-2 Level 1C data can be accessed directly through the Google Earth Engine catalogue and imported into the code editor for processing in the cloud. GEE has successfully integrated the Sentinel-2 Level-2 data from Copernicus SciHub in their catalogue, which has been computed by the sen2cor processor. However, as mentioned earlier, Level 2A data has not been produced for all Level 1C assets and depending on the area of interest, it is possible not find sufficient Level 2A data available.

A big limitation in using optical data in region like the Colombian Pacific coast is that many images are obscured partially or almost entirely by clouds. A solution for this is to apply a cloud masking algorithm. The algorithm is applied to each image to evaluate the probability of each pixel being a cloud. Every pixel of the image that is deemed cloud-free will be kept, and cloudy pixels will be converted to “no data” areas. Then, the remaining patches of the images are combined into a mosaic. Rather than combining several images into a bigger one, multiple images covering the same region will be stacked together. In this way, there are higher chances of having pixels with no data filled in by pixels with data from other images, and ideally getting a full cloud-free composite.

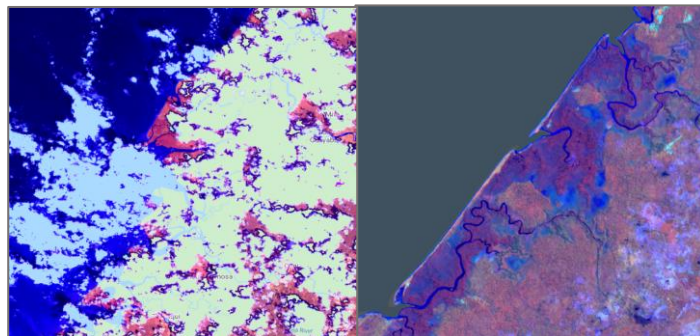


**Fig 9.** Comparison between Sentinel-2 masked image (false-colour) and a median composite generated from all masked images for an area presenting mangrove cover (darker purple) (Google basemap)

Elements like haze, thin cirrus and cloud shadows are not easy to detect (Sudmanns et al. 2020), and therefore, different cloud masking options were explored to find the optimal solution to generate cloud-free composites in the study area. There is no perfect solution of course and the task can be considerably challenging.

## Cloud and shadow masking algorithms

There are different methods applicable in GEE for obtaining a cloud free composite. Three major cloud masking algorithms used for Sentinel-2 images are sen2cor, FMask and S2cloudless. Sen2cor is the algorithm applied by the European Space Agency (ESA) to derive cloud and shadow masks. Within the GEE repository the cloud mask product is provided with the S2 L2A (SR) product. This means that the S2 Level 2A data cloud masking can be executed directly in GEE using the Sentinel-2 Cloud Probability product also available in their catalogue. However, according to some studies (Coluzzi et al. 2018; Sudmans et al. 2020), ESA's cloud detection algorithm is not accurate for all regions and cloud cover situations. FMask, on the other hand, is the method used by the US Geological Survey (USGS). Some researchers have argued that it works better than sen2cor, but others consider that it is designed more for Landsat, and that large temporal and spatial ranges can be detected missing when using Sentinel-2 data (Nagy, 2021). Finally, S2cloudless is an algorithm applied by Sentinel Hub and has been recommended by some over sen2cor.

An alternative option to the ones already introduced is the cloudScoreTDOMShift method, which was the cloud masking approach applied in this study, based on Shapiro et al, (2015). It is an adaptation of the ee.Algorithms.Landsat.simpleCloudScore() routine in GEE, achieved by selecting the appropriate bands from Sentinel-2 to align with the original Landsat bands, and adjusting the classification thresholds to account for these differences. The principle of the algorithm is to recognize that clouds are bright, moist, and not the same as snow (Schmitt et al. 2019). The parameter values applied by Shapiro et al (2015) in their script was adapted to the study area with the support of other studies (Candra et al, 2017, Shapiro et al, 2018). Parameter adjustments needed to be made since the values that were used in other studies did not perform well enough in the study area. For instance, by lowering the cloud threshold, the presence of cloudy and/or hazy pixels in the image was reduced (Fig 10)

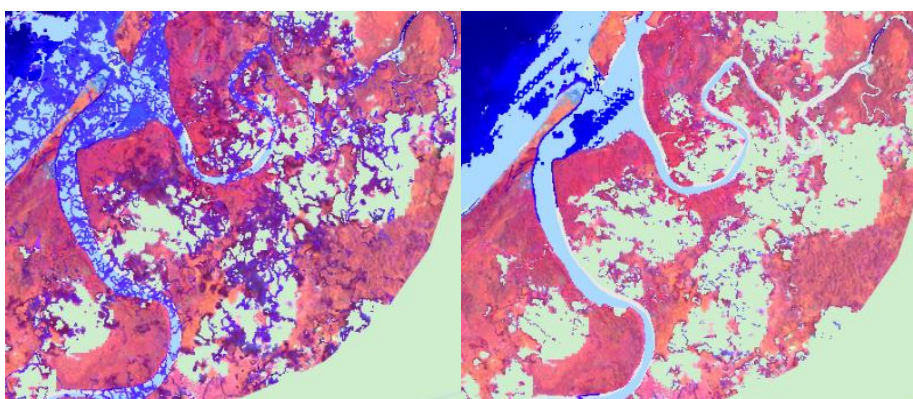


**Fig 10.** Comparison between Sentinel-2 masked image (false-colour) with different parameter settings (false-colour) (Google basemap)

The final selection of values was made according to visual inspections of the results, following expert recommendations. The final parameter values that were used for the TDOM algorithm are included in Table 7.

**Table 7.** Ancillary data used during the classification process.

Parameter	Value	Description
<b>dilatePixels</b>	1.5	controls the number of pixels used to buffer clouds and cloud shadows
<b>cloudHeights</b>	ee.List.sequence (200,5000,250)	the height of clouds to use to project cloud shadows.
<b>zScoreThresh</b>	-1	the threshold for cloud shadow masking, a lower number will mask out fewer pixels. Default value should work well for most areas
<b>shadowSumThresh</b>	3500	the sum of infrared bands to include as shadows within the dark object method, TDOM, and the shadow shift method. A lower number will mask out fewer pixels.

### Sentinel-2 Median Composite

While masking clouds and shadows eliminates much of the noise in the data, many artifacts are likely omitted in the masks. Since artifacts are likely to be outliers, after the filtering and cloud/shadow masking was performed, the median reducer was applied to create a composite with a reduced likelihood of including those outliers (Housman et al. 2015). The result can be seen in Figure 11.

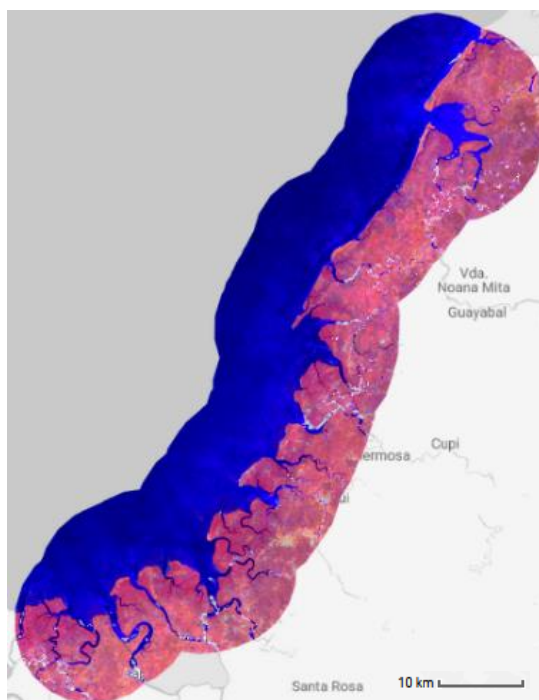


**Fig 11.** Sentinel-2 masked median composite (false-colour) (Google basemap)

## Greenest pixel composite

An additional option considered, which has been also widely used as an alternative for cloud removal, is applying quality mosaic algorithm, in this case GEE's `qualityMosaic()` routine. The quality mosaic operates on a pixel-by-pixel basis. For each pixel location, it goes through the entire collection and selects the pixel with the highest quality score in that location. In other words, rather than prioritizing the least cloudy image, it prioritizes the pixel with the “greenest pixel”, or highest NDVI value in this case. One of the drawbacks of this is that the resulting image may contain two adjacent pixels that come from wildly different images, if those pixels had the highest Quality Score. So instead of masking, which involves removing data, the “quality mosaic” scans the quality of all the pixels in all the images and selects the pixels with highest NDVI values regardless of how cloudy the image as a whole might be (Nagy, 2020). This option was used to compare the performance of a less computationally complex alternative for creating cloud-free composites, to be used in the classification of mangroves, against the results from using the TDOM-masked composites. Figure 12 provides the “greenest pixel” composite result.

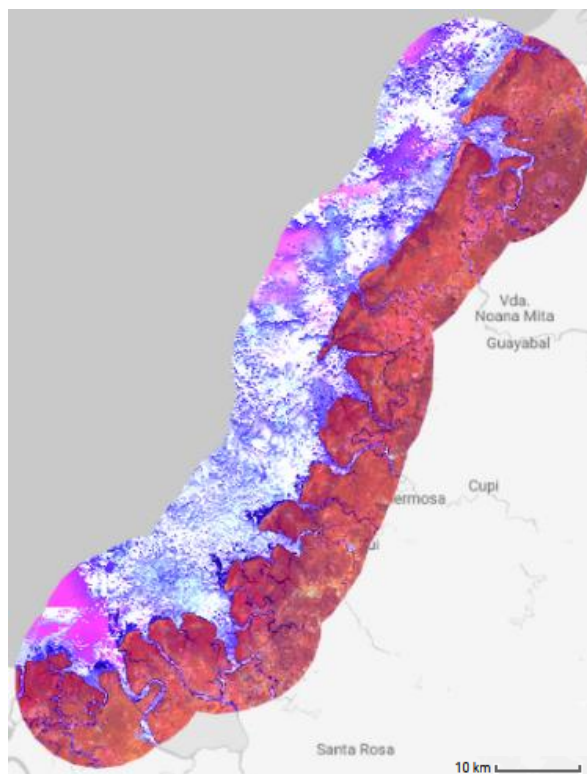


**Fig 12.** Sentinel-2 “greenest pixel” composite (false-colour) (Google basemap)

At this point we have two “cloud-free” images, one obtained by applying the TDOM and the other based in the “greenest pixel”. The next step was to generate the index bands that would be used in the classification.

## Spectral index selection and calculation

After the cloud-free Sentinel-2 composites were ready several indices were calculated and stacked with the original composite bands. The indices used were based on selections and recommendations made by different studies (Wang et al., 2018; Shapiro et al., 2018; Muhsoni, 2020; Yancho et al 2020). All indices were calculated within GEE for the year 2020.

For this study 12 indices (SR, R48, R118, NDVI, CMRI, MMRI, NDMI, MVI, NDWBI, MNDWI, OSAVI, LSWI) were generated, four of which are mangrove-specific. The selected indices were calculated for both the masked-median mosaic and the greenest-pixel mosaic and stacked as classification inputs. Figure 13 compares the appearance of a typical mangrove-dominant area in the Cauca department across selected mangrove-specific spectral indices (i.e. CMRI, MMRI, MVI, NDMI) (Diniz et al. 2019; Zhang et al. 2013; Gupta et al. 2018; Baloloy et al 2020; de Sousa et al., 2020). The list of all indices tested can be found in the GEE scripts provided in the results section. The indices used in the classification model were selected from the workflows of Shapiro et al. (2015) Shapiro et al. (2018), and Yancho et al (2020).

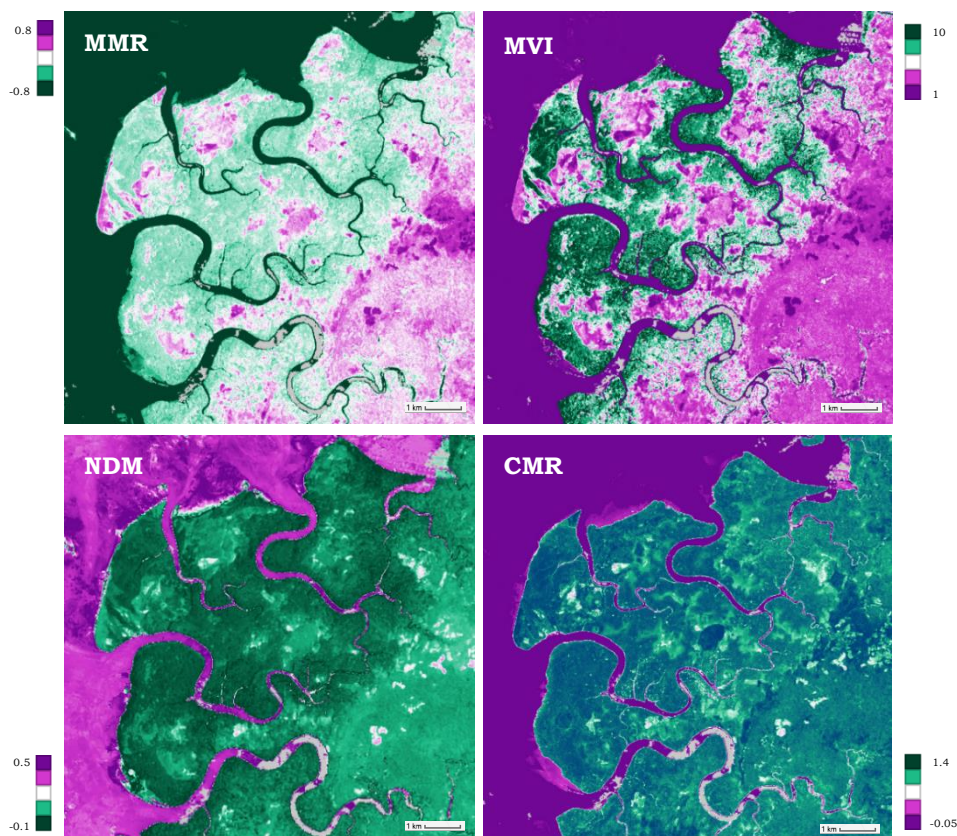


**Fig 13.** Mangrove-specific indices (CMRI, MMRI, MVI, NDMI) applied to a mangrove-dominant area in the Cauca department.

The final products included two composites with 10 bands each, from which the indices listed in the table 8 were calculated and stacked with the Sentinel-2 bands.

**Table 8.** Indices used in the classification model

<b>SR</b>	Simple ratio
<b>R48</b>	Red/Nir band ratio
<b>R118</b>	Swir/Nir band ratio
<b>NDVI</b>	Normalized Vegetation Index
<b>CMRI</b>	Combined Mangrove Recognition Index
<b>MMRI</b>	Modular Mangrove Recognition Index
<b>NDMI</b>	Normalized Difference Mangrove Index
<b>MVI</b>	Mangrove Vegetation Index
<b>NDWBI</b>	Normalized Difference Water Band Index
<b>MNDWI</b>	Modified Normalized Difference Water Index
<b>OSAVI</b>	Optimized Soil-Adjusted Vegetation Index
<b>LSWI</b>	Land Surface Water Index

## 5.2.2 Sentinel-1 pre-processing

### Sentinel-1 Pre-processing

Sentinel-1 radar data pre-processing is more complex than multispectral data pre-processing. All the steps taken were based in Shapiro et al. (2015) workflow and GEE scripts, with the support of additional studies (Filipponi, 2019; Vasquez, 2019). The procedure was adapted to the study area, in terms of adjusting filtering and making parameters as well as some structural modifications and additions. The GEE platform was used to process all Sentinel-1 data and to calculate the metrics from the VV and VH bands (20th, 80th percentiles, standard deviation and VH/VV ratio) based on the workflow by Shapiro et al (2018). The temporal window used was the same as for the Sentinel-2 processing. The final product consisted of one composite with all bands.

### Data filtering

The Sentinel-1 GRD (COPERNICUS/S1\_GRD) product is available in the GEE repository and can be directly imported to the code editor for processing. First the collection needed to be filtered meet the year, area, swath mode, polarizations, and orbit direction of interest. The choices were made in support of other studies (Portengen, 2017; Vasquez, 2019, Filipponi, 2019). The collection was filtered to include all images for the year 2020 and to the bounds of the final ROI, which was pre-defined in the initial steps of the analysis. The data was collected using an Interferometric wide swath mode of both the VH (vertical transmit-horizontal receive) and VV (vertical transmit-vertical receive) polarizations and in ascending orbit

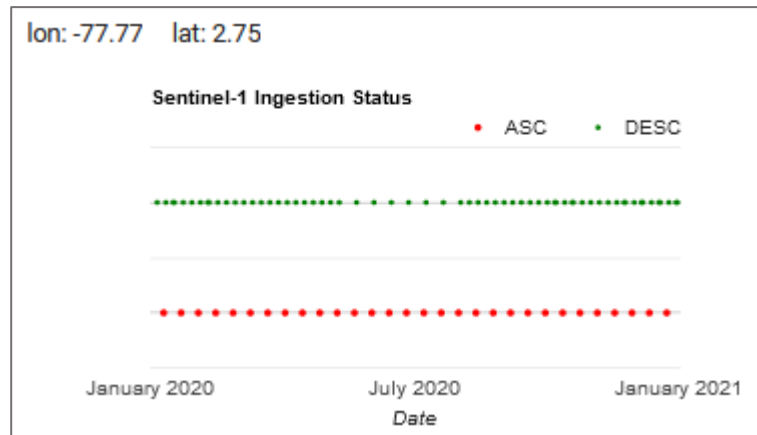


**Fig. 13** Sentinel-1 Ingestion status

The VH polarization is more sensitive to changes on the land surface, and is commonly used for flood mapping, while the VV polarization is more sensitive to vertical structures and may be useful to delineate open water from land surfaces. The images collected in ascending orbit had a better temporal distribution compared to the descending orbit.

For visual comparison both bands were set into the same contrast stretch in the colour manipulation settings so that they represent the same value ranges, in this case -25 to 0 dB. When visually comparing the VH band image with the VV band image, it is quite apparent that the VH image shows lower values than VV image. This effect is caused of lower backscatter in general (Flores et al., 2019)

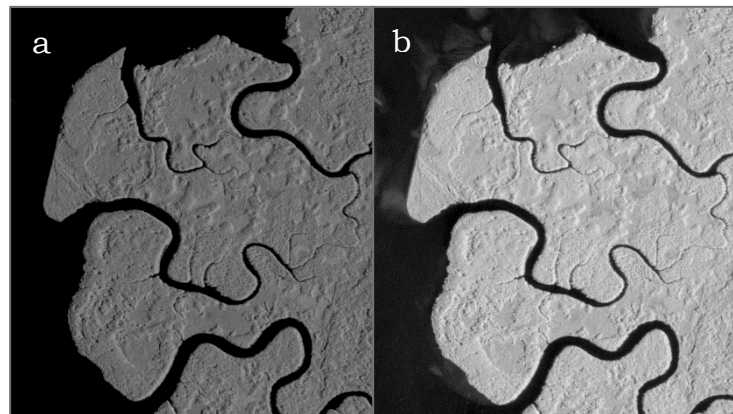


**Fig 14.** a. VH median, b. VV median (Sentinel-1 GRD images)

### **Speckle and noise removal**

A common approach to reduce the effect of noise and outliers is to apply Speckle filters and averaging methods. The Sentinel-1 C-band is sensitive to the scattering elements and their electromagnetic characteristics. A forest will likely receive a more direct scattering radiation, hence, a higher backscatter, than other types of landcover, such as grasslands or water bodies. The later will tend to scatter a more incident radiation from the sensor. In order to minimize the speckle and noise effects caused by extreme backscattering, temporal averaging was applied for the entire year by selecting all available images of the



year 2020 and calculating the median of pixels. By applying an averaging operation such as the median, the effect of soil moisture in the power of SAR is also greatly reduced (Xu and Wang, 2020). The choice of median rather than the mean backscatter per pixel was supported by different studies which consider it be more robust against extreme values than the mean (Anaya et al, 2020; Reiche et al. 2018; Mahdianpari et al., 2018). Moreover, the azimuth and range compression lead to radiometric artefacts at the image borders. Thus, a border noise removal algorithm was also applied to remove low-entropy edges and invalid data on the scene edges (Filipponi, 2019).

The next step was to filter the temporal speckle noise from the time series data (Filipponi, 2019; Xu and Wang, 2020). Speckle, which appears in the SAR images as granular noise, is caused by the interference of waves reflected by the scattering elements (Filipponi, 2019). Speckle filtering will increase the quality by reducing speckle, so that it will not be propagated in the ongoing processes (i.e., terrain correction or dB conversion). The structural information in the radar backscatter is important, particularly when used in the vegetation biophysical modelling (Ananto et al. 2019). Thus, the choice of speckle filtering, must be applied on a case-by-case basis, and may be not recommended if small spatial structure identification is of interest, since it could remove such information. Due to the different processing implemented between the filtering methods, the ability in preserving the structural information contained in the backscatter signal should be studied (Ananto et al. 2019). Although Refined Lee filter is a commonly used method (Filipponi, 2018), after reviewing studies applying speckle filter to Sentinel-1 SAR images for mangrove cover areas specifically (Shapiro et al, 2015; Vasquez, 2019, Senthilnath et al. 2013) the Maximum A Posteriori Probability Filter (Kuan et al. 1987), or Gamma MAP filter was preferred. Thus, after performing a visual comparison between Refined Lee and Gamma MAP, the later was applied.

The Gamma-MAP filter combines geometric and statistical properties to produce the DN values of the pixel and the average DN of neighbour pixel using moving windows. The number of looks was set to 5 looks considering the image scale of 10m and based on the workflow of Aurelie et al, (2018). The after performing a visual comparison between 3x3, 5x5 and 7x7 window sizes, the filtering window was set to 5x5 to minimize noise present in the original image, while preserving some detail, considering that the 7x7 kernel was heavily generalizing the image, and the 3x3 kernel size was not generalizing enough (Vasquez, 2019). As a final step, the backscatter coefficient was converted to dB using a logarithmic transformation (Ananto et al. 2019).

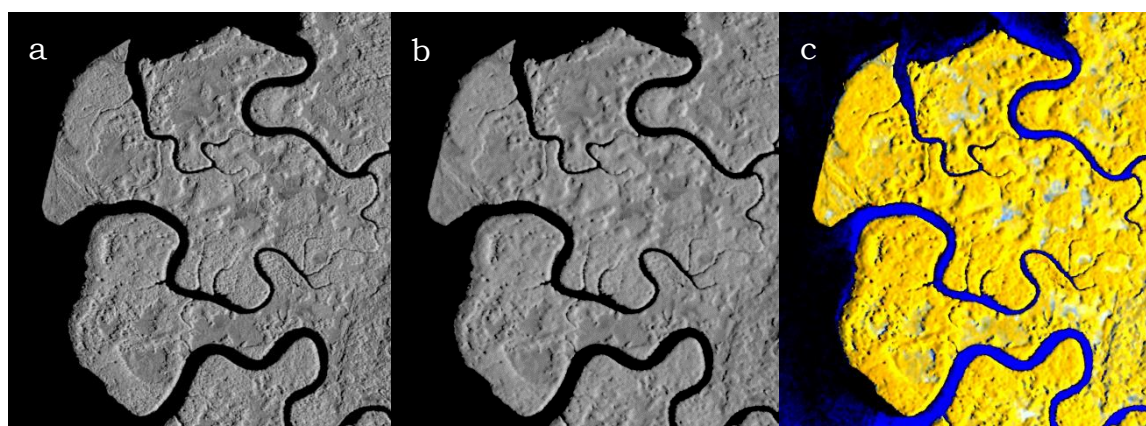


**Fig 15 a.** Gray scale S1 VV median image without speckle filtering in a mangrove-presence section in the Cauca department, (-25 to 0 dB); **b.** Gray scale S1 VV Gamma MAP 7x7 filtered image for the same section (-25 to 0 dB); **c.** Median backscatter composite of band polarizations VV, VH and VH/VV with the visible effect of temporal averaging, in the same section.

### Water occurrence and mask

Since optical data can present limitations due to its inability to penetrate cloud cover, the use of Sentinel-1 SAR data was considered in this study to mask out water. Quantifying water extent through S1 data has been considered to have advantages over optical sensors in quantifying spatio-temporal variation of water extent by different studies (Huang et al. 2018; Lang et al, 2015; Cazals et al. 2016). These advantages include collecting information day-and-night and in all weather conditions. Also, sensitivity to both open water and inundation bellow canopy (Huang et al. 2018). Using SAR backscatter for detecting surface water relies in the fact that water bodies, being open and smooth, will typically exhibit lower backscatter coefficients (Brisco, 2015).

The water threshold was calculated using Otsu’s classic thresholding method (Otsu, 1979). This method applies a thorough search for the threshold that minimizes the weighted sum of variances of change and background classes (Xu and Wang, 2020). Otsu’s method has a good performance in the study area, considering that the histogram showed a bimodal distribution and a sharp valley between two peaks (Xu and Wang, 2020). The variable threshold is recalculated for each image and then the water mask is determined. Water occurrence (Figure 16) was calculated and displayed (0%-no occurrence, 100%-always water present), based on the workflow developed by Buttig (2020). Apart from deriving the water mask, displaying water occurrence was helpful to understand the behaviour and variation in water presence along the coastline, which could influence the detection of mangroves.

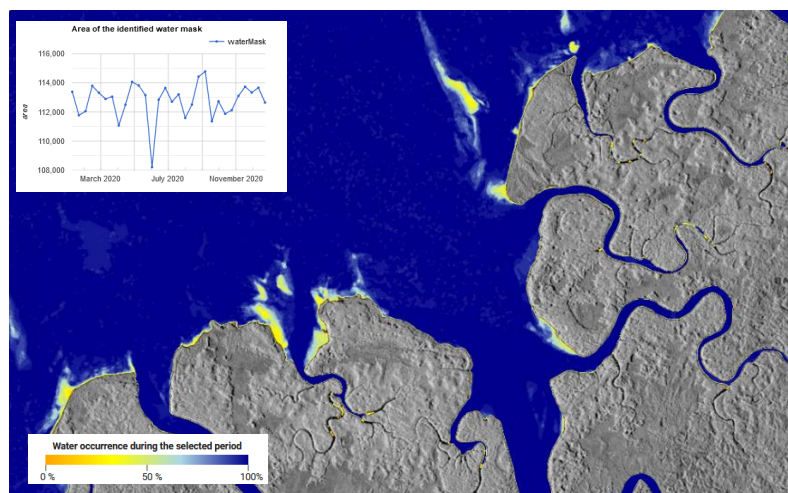


**Fig 16.** Water occurrence from Sentinel-1 collection

The fact that the study area is characterized by being very cloudy, was the main incentive for using the S1 SAR data for water masking rather than the S2 data. Generally, water masking is performed effectively using the Sentinel-2 data, as has been demonstrated by many studies (Shapiro the al., 2015; Shapiro et al. 2018). Water masking was also analysed using the Sentinel-2 composites (masked median and greenest pixel), by also applying Otsu's automatic threshold method and the Normalized Difference Water between green and NIR (NDWBI) (Shapiro et al, 2018). The index was developed to detect water pixels by calculating the normalized difference between the green and the near infra-red band, making it suitable for measuring the amount of water present in an acquisition.



**Fig 17.** Comparison between Sentinel-2 water mask applied to greenest pixel composite (first image), S2 water mask applied to the median masked image (second), and Sentinel-1 water mask (third) (Google basemap)

As was expected, the water masking using the greenest pixel composite did not perform well. Extracting the greenest pixels over water bodies introduces colour artifacts for water surfaces, which affect the spectral behaviour of such bodies and limit its detection using a threshold. As for the median, although it was quite successful for mask out water, missing data patches were present corresponding to masked out areas during the cloud and shadow masking process. Therefore, the Sentinel-1 water mask provided a greater coverage and was considered overall more consistent option for the classification.

## 5.3 Classification

### 5.3.1 Supervised classification

Supervised classification can be implemented using different classifiers (SVM, CART, Random Forest, etc). Within the GEE environment some of these classifiers have already been built in, which include the Minimum Distance, Classification and Regression Trees, Support Vector Machine and Random Forest. Some of them are relatively straight forward, and some require a manual input decision tree. In general, the process works by assigning a class to a set of pixels in the image, called training pixels, and a classifier will be constructed and applied to the rest of pixels to automatically or semi-automatically classify them. From this, the extent of the land cover of interest can be extracted.

Based on the recommendations of various studies (Portengen, 2017; Pimple et al., 2018; Mondal et al., 2019; Tieng et al., 2019; Gilani et al., 2020), the Random Forest classifier was chosen for performing the classification. The Random forest algorithm (Breiman 2001) operates by executing multiple decision trees, which are independently produced, and each node is split using a chosen number of features. RF takes the training areas, samples them against the different spectral bands and indices and then uses a random sampling scheme to assign pixels into classes of mangrove and non-mangrove.

Training data were identified from existing maps (Giri et al. 2011; Global Mangrove Forest Watch 2016, Simard et al. 2019) together with visual identification and field information (UAV data). The training image was prepared by masking out water, based on the mask generated in the Sentinel-1 pre-processing stage, as well as elevation (m) and slope (%) based on automatically calculated topographic thresholds. The thresholds were generated by extracting the 99th percentile values from within the known mangrove extent dataset (Simard et al. 2019) based on the workflow by Yancho et al. (2020) and Fatoyinbo et al. (2018). For the Cauca department the masking thresholds were  $> 44\text{m}$  (elevation) and  $>23$  (slope). The elevation threshold, which is based on the ALOS PALSAR DSM (30m), represents an approximate elevation and canopy combined height, past which mangroves are not found (Yancho et al. 2020). All masks were combined and applied to the composites within the defined ROI.



**Fig 18.** Elevation mask (Also PALSAR DSM) (displaying range between  $-5\text{m}$  to  $44\text{m}$ ) (Google basemap)

The number of trees must also be defined. A larger number of trees is generally thought to provide more accurate results, since each decision tree will generate a class result from which the majority is chosen, but at the expense of computation times (Portengen, 2017). According to an investigation on the sensitivity of number of trees by Belgiu et al. (2016), smaller values can also deliver good results, in addition to shorter computation times. Considering that the image was going to be classified based on two classes only, mangroves and non-mangroves, and supported by other related research studies (Shapiro et al. 2014; Portengen, 2017) the number of trees was set to 50. This value provided good results, and computation times that Google Earth Engine was able to handle.

### 5.3.2 Training sites and validation data

Training and validation data were produced through a random stratified design based on the workflow of Shapiro et al. 2015 and supporting research (Portengen, 2017; Anaya et al., 2020; Shapiro et al., 2018). Two classes were defined: mangrove and non-mangrove. Thus, polygons of known areas of mangrove and non-mangrove were drawn into the maps and used as samples for the classification.

The selection of training sites was supported by an integration of multiple information sources, that indicated the presence of mangroves. Support data included: reference mangrove maps (GMW2016 and Hmax95), field data (UAV images for the year 2019) and official reports from local institutions (Invemar, 2015) providing information on the location of mangrove forests.

Visual interpretation was made easier by creating false-colour composites (Vasquez, 2019; Anaya et al., 2020; Purwanto and Asriningrum, 2019) that differentiated the land covers more clearly. False-colour composites can greatly help in identifying mangrove cover, however, the process of deriving the optimal band combination can take a considerable amount of time due to many combinations possible (Purwanto and Asriningrum, 2019). Therefore, different studies were consulted to derive a band combination that highlights mangrove cover. These studies agree that the best Sentinel-2 band combination for identifying mangrove forests from surrounding colour is Vegetation Red Edge + SWIR + Red (8A-11-4) (Purwanto and Asriningrum, 2019; Vasquez, 2019; Aurelie Shapiro et al., 2018). With this band combination mangrove areas appear in a darker red tone. Therefore, this band combination was used to generate a false-colour composite that would aid in distinguishing mangroves in the Colombia Pacific coast.

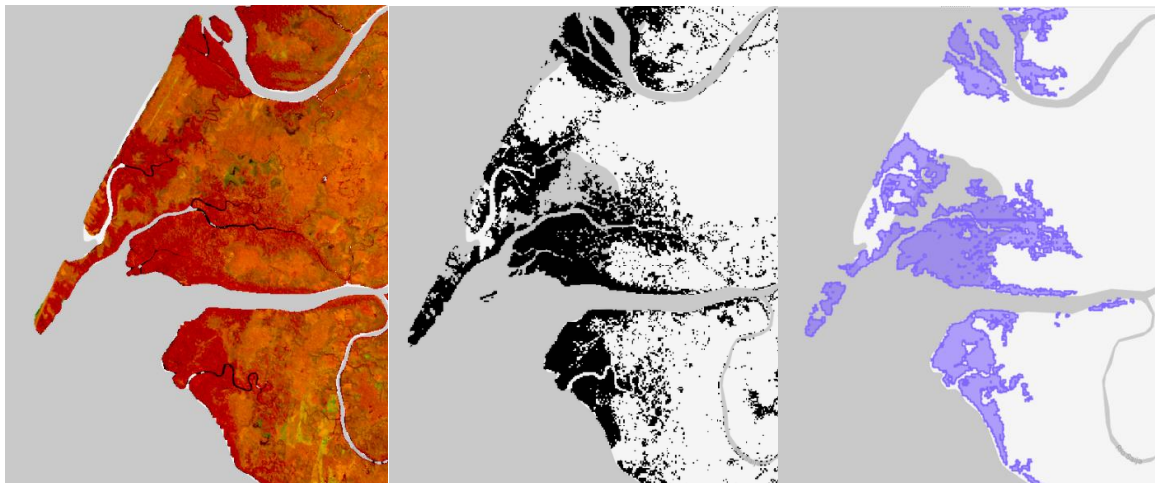


**Fig 19.** False-colour composite (bands 8A-11-4)(first image), Hmax95 mangrove dataset (Simard et al. 2019) (second image) and Global Mangrove Watch 2016 dataset (third image) (Google basemap)

Overall, priority was given to those sites that presented the least uncertainty, and since the Colombian Pacific coast presents a high variety of mangrove species (8 mangrove-exclusive species) attention was invested in selecting a high variation of training sites. Some mangroves are more shrub-like (e.g. *Avicenia germinans*) in nature while others

are more tree-like (*Rhizophora mangle*), which could potentially affect classification if there is not a good enough variety of training sites.

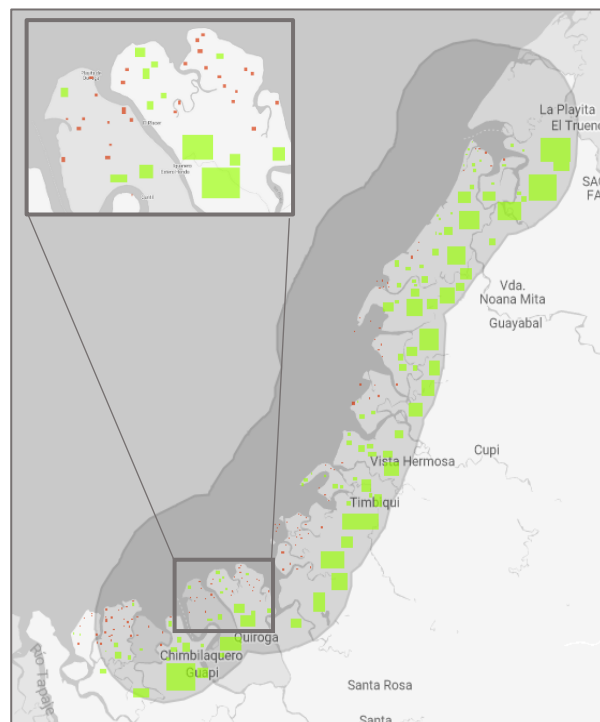


**Fig 20.** Training polygons (green for non-mangrove, and red for mangrove sites) (Google basemap)

From the drawn polygons a total of 1000 training points and 500 validation points was randomly generated for each class. These represent ground-truth data. Due to the random generation of points, every time the classification algorithm is executed the results can change slightly (maximum by 1%) (Portengen, 2017). By reducing the number of validation points, the chances of overlapping training and validation points was also reduced (Anaya et al. 2020). Nonetheless, a visual inspection was performed to make sure training and data points did not overlap.



**Fig 21.** Light grey showing training points, black showing validation points. (Google basemap)

### 5.3.3 Classification models

After stacking all the bands together and masking out elevation and water, the training image was generated. A training image is needed for the polygons to serve as input on the classification algorithm, samples from that image will be taken based on the polygon’s location properties. In order to determine the best sensor and variable combination to map mangrove forests, 4 models were developed, consisting of combinations of Sentinel-1 and Sentinel-2 imagery (Table 9).

**Table 9.** The four combinations of the models tested

Model	Sensor	Data included
1	Sentinel-2 (median masked)	All bands and indices
2	Sentinel-2 (greenest pixel)	All bands and indices
3	Sentinel-1	All bands
4	Sentinel-1 and Sentinel-2	All bands and indices

The random forest algorithm took the training areas defined earlier, sampled them against the spectral bands and indices, and applied a random sampling scheme to assign the pixels into either the mangrove class or the non-mangrove class. The classification was executed for the year 2020 and the results were filtered to remove small individual pixels and noise, setting the minimum area to 1ha, based on the workflow by Shapiro et al. (2015). First the classification algorithm tested on each of the Sentinel-2 models, masked median and greenest composite. Then, the algorithm was run on the Sentinel-1 model and finally, applied to test the Sentinel-1 and Sentinel-2 combined data model. The results using the different inputs was compared both quantitatively and qualitatively, and finally the best solution was chosen for running it over the entire pacific coast. All

mangrove patches less than 1 hectare were reclassified to match the surrounding class. The resulting classification was set to a minimum unit of 1 ha and was masked to a buffer of 1 km from the edge of the reference mangrove layer (Hmax95 dataset from Simard et al, 2019), in order to estimate the extent and distribution of core mangrove areas and reduce overestimation. (Shapiro et al. 2015).

### **5.3.4 Temporal and spatial transferability**

Considering the resulting accuracies and mangrove spatial distribution obtained from the pilot study, the classification model was selected for classifying the rest of the Colombian pacific coast, by department, and a different year (2017). The departments were classified independently, one by one, to reduce computation time, as the coastline is very extensive and would produce constant time-outs. Most effort was needed for the Nariño and Chocó departments, due to their extents. Nariño is the department with the biggest mangrove cover extent, by far, and in some areas, it goes more than 30km inwards from the coastline, while for others it was less than 10 km. This meant that the derived ROI size was quite large, and longer computation times were required for each step, often leading to time-outs. The Chocó department, on the other hand, has the longest coastline and the classification presented mangrove patches towards the north that had not been included in the reference mangrove maps. Therefore, the reference mangrove buffer for masking classification area was not used for classifying the Chocó department, in order not to omit them. However, the calculated distance from the coastline (10km in the Choco case) required for delimiting the ROI and the elevation data for masking were good enough for this department.

In terms of applying the model with imagery from a different year, the 2017 year. This year was chosen because it is the furthest year from 2020 in which already both Sentinel-2A and Sentinel-2B were in orbit. Hence, assuming that the revisit time for most of the year 2017 would be similar to that of 2020. From the resulting classification, a mangrove cover change analysis was then performed to evaluate the possibility of using the model also for monitoring mangrove extent dynamics, from year to year. The results were then integrated and published as a GEE app for a better visualization experience.

### **5.3.5 Validation and accuracy assessment**

The previously defined validation points were used to check if they coincided with the resulting classes after the procedure had been run. The accuracy assessment is an essential part of image classification as it quantifies the validity of the results. In this study a total of 500 points per class were used for validation, which provide the quality of data information to be assessed. The accuracy was calculated together with the size of the area covered by the mangrove cover class in the derived classified map. These results also guided the choice of input data to use in the final classification model.

A commonly used method for expressing the classification accuracy is the confusion matrix (or error matrix). The confusion matrix compares the relation between the validation (ground truth) data and the corresponding classification results. The matrix



calculates all adjacent values and coefficient. By dividing the number of accurately classified pixels by the total number of pixels, the overall accuracy will be calculated.

Additionally, the confusion matrix includes the user's and producer's accuracies. The producer's accuracy is calculated by dividing the total number of pixels accurately classified by the total number of pixels of each input training class. The user's accuracy on the other hand, is the division of the total number of correctly classified pixels by all the pixels classified for each class in the classified image. Both accuracies are adjusted to the amount of validation pixels per class, so that a class with more available pixels does not automatically get higher accuracy values (Portengen, 2017).

Moreover, a qualitative comparison with the drone (UAV) images was performed. Although this was only available for small patches along the pacific coast, it is an additional way to do a classification quality check and asses how accurate the Sentinel-2 data results are compared to high resolution data information. Three drone images were accessed from field work performed by a local expert each from a different department (Chocó, Valle del Cauca and Nariño) representing a small sample from the north, centre and south of the pacific coast.

### **5.3.6 Results**

All the models achieved accuracies between 90% and 97%. Considering the conditions of the region, the annual composite-based models performed better than expected and were able to map mangrove cover quite accurately. Comparing the two different sensors alone, Sentinel-2 models outperformed the Sentinel-1 model. Although the Sentinel-1 model was able to distinguish mangrove cover quite well, it has a higher tendency to misclassify non-mangrove pixels into mangrove pixels, which was reflected in the 75% producer's and consumer's accuracy for that class. This resulted in an overestimation of mangrove cover, which can also be visually noted (Figure 24).

When combining Sentinel-1 and Sentinel-2 data the model produces a very slight (less than 1%) increase in the producer's and consumer's accuracies for both classes. However, it was not significant and visually the maps are quite similar. For this reason, considering that the effort required for the more complex combined model and the masked sentinel-2 model is much larger, and provides a minimum gain, the selected model for performing the classification of the entire pacific coast was the model using de Sentinel-2 greenest pixel composite. All indices were also included as classification variables.

The results from each of the models applied to the pilot study area, Cauca department, are presented here, both in terms of their spatial distribution along the coast, including their extent estimates, as well as the resulting accuracies. A land cover map produced from these models is shown in Figure 23, with the associated accuracy statistics and mangrove area estimations in Table 10.

**Models 1 and 2 (Sentinel-2 only + indices)**

The Sentinel-2 model incorporating the median masked composite had an overall accuracy of 96.9%, whereas the Sentinel-2 model incorporating the greenest pixel composite has an overall accuracy of 96.7%. A land cover map produced from these models is shown in Figure 22 and Figure 23, with the associated accuracy statistics and mangrove area estimations in tables 10 and 11.

Sentinel-2 masked median model

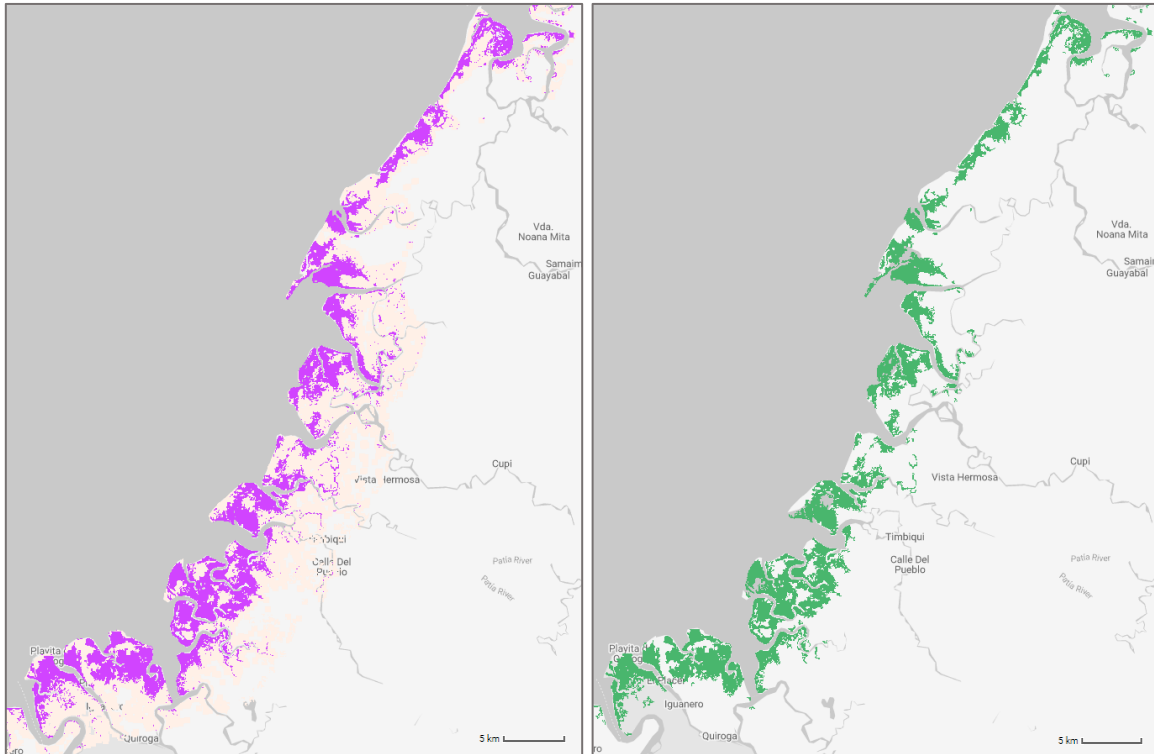


**Fig 22.** Resulting mangrove distribution from the median masked model. Before applying the 1ha minimum size (pink) and after masking the mangrove class and removing <1ha patches (green) (Google basemaps)

**Table 10.** Accuracies for the S2median masked model

Sentinel-2 (masked median)	Accuracy results		
	Producer's	User's	Overall
mangrove	0.977	0.980	0.969
not mangrove	0.944	0.939	
Extent	17,846 ha		

Sentinel-2 greenest pixel model

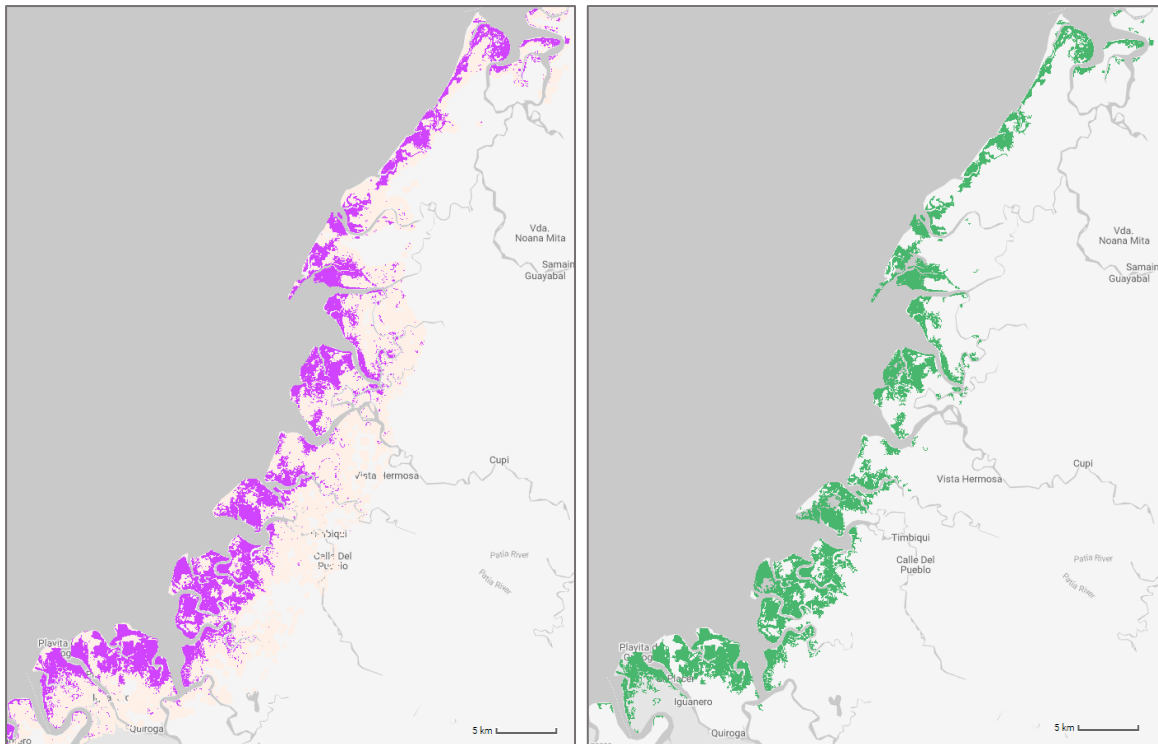


**Fig 23.** Resulting mangrove distribution from the S2 “greenest pixel model”. Before applying the 1ha minimum size (pink) and after masking the mangrove class and removing <1ha patches (green) (Google basemaps)

**Table 11.** Accuracies for the “greenest pixel model”

Sentinel-2 (greenest)	Accuracy results		
	Producer’s	User’s	Overall
mangrove	0.967	0.977	0.967
not mangrove	0.939	0.939	
Extent	17,805 ha		

### Model 3 (Sentinel-1 only + indices)

The Sentinel-1 model had an overall accuracy of 90.2%. A land cover map produced from this model is shown in Figure 24, with the associated accuracy statistics and mangrove area estimation in Table 12

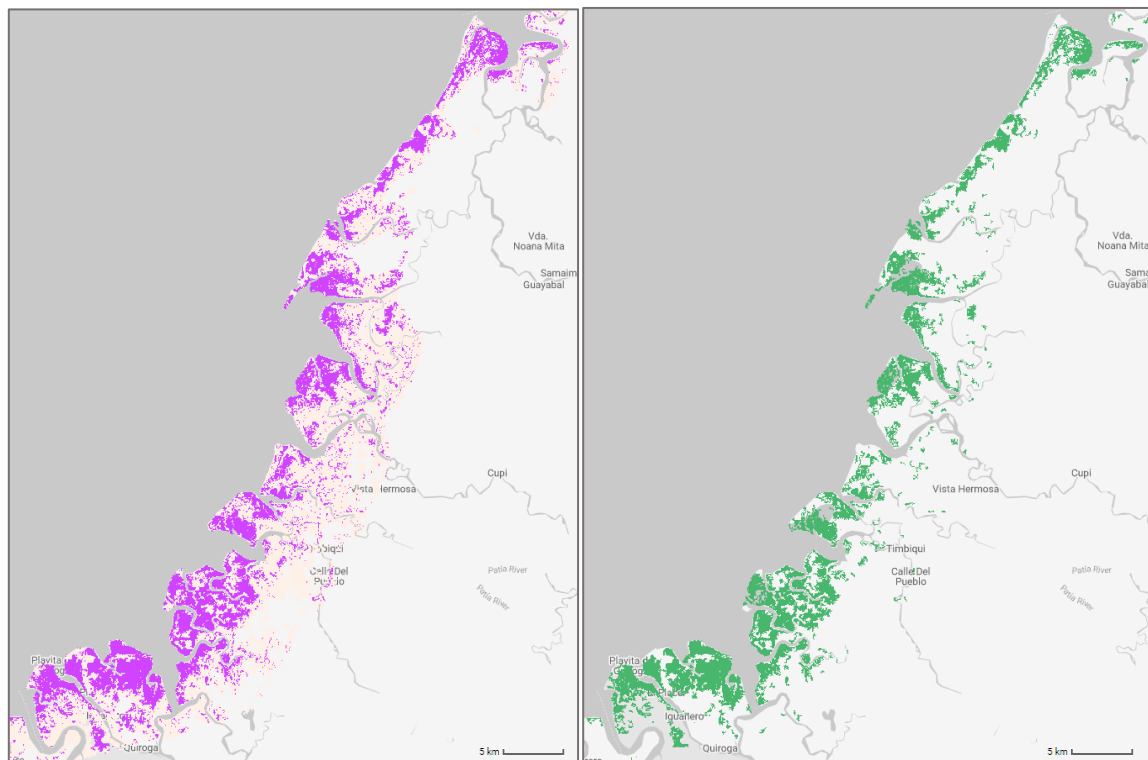


**Fig 24.** Resulting mangrove distribution from the Sentinel-1 (only) model. Before applying the 1ha minimum size (pink) and after masking the mangrove class and removing <1ha patches (green) (Google basemaps)

**Table 12.** Accuracies for the Sentinel-1 (only) model

Sentinel-1	Accuracy results		
	Producer's	User's	Overall
mangrove	0.957	0.913	0.902
not mangrove	0.75	0.866	
Extent	20,038 ha		

#### Model 4 (Sentinel-1 + Sentinel-2 + Indices)

The combined (S1+S2) model had an overall accuracy of 97.3. A land cover map produced from this model is shown in Figure 25 with the associated accuracy statistics and mangrove area estimation in Table 13.

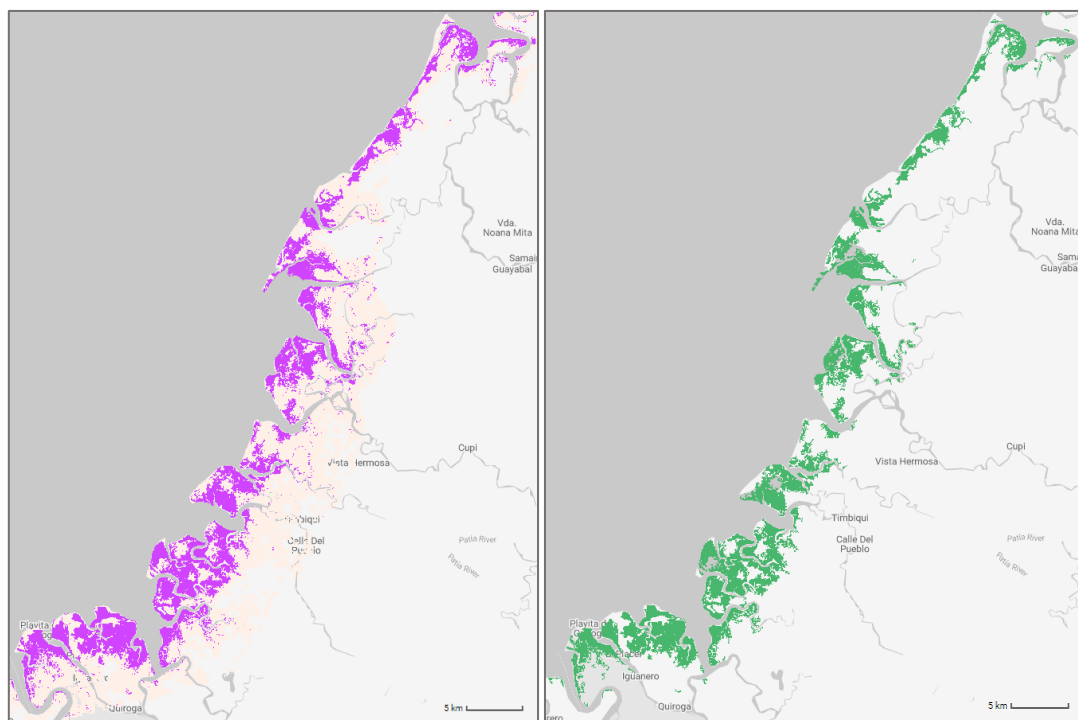


**Fig 25.** Resulting mangrove distribution from the combined (S1+S2) model. Before applying the 1ha minimum size (pink) and after masking the mangrove class and removing <1ha patches (green) (Google basemaps)

**Table 13.** Accuracies for the combined (S1+S2) model.

S1 and S2 combined	Accuracy results		
	Producer's	User's	Overall
mangrove	0.98	0.95	0.973
not mangrove	0.95	0.98	
Extent	17,694 ha		

#### Transferability to a different year and location

As stated before, taking into consideration the resulting accuracies and mangrove extents obtained from the pilot study, the selected model for classifying the rest of the Colombian pacific coast and a different year, was the Sentinel-2 greenest pixel model. Despite what was initially expected, the greenest pixel provided almost the same accuracy than the median masked model and using Sentinel-2 imagery (and the calculated indices) alone was enough to map mangrove forests in the pacific coast.

The model was tested for the different departments and for the year 2017 to assess its performance in a different spatial and temporal context. The extent and accuracy results for each of the departments for the year 2020 can be found in Table 13. The model was also applied for the year 2017, only for the department of Cauca, in order to assess its performance, rather than focusing on change detection over the entire Colombian pacific coast. The overall accuracy for that year was 97% and the extent was estimated to be 16,370 ha, compared to the 17,805 ha for the year 2020. This meant that according to the model results there was an increase of 1,435 ha between both years.

**Table 14.** Extent and accuracy results for each of the departments for the year 2020

<b>Department</b>	<b>Year</b>	<b>Overall accuracy</b>	<b>Mangrove extent (ha)</b>
Chocó	2020	0.96	42,651
Valle del Cauca	2020	0.92	29,688
Cauca	2020	0.97	17,805
Nariño	2020	0.97	106,534

### **Visual qualitative comparison with UAV images**

The Sentinel-2 satellites are equipped with sophisticated sensors providing high spatial, temporal, and radiometric resolutions, aligned with extensive coverage that have widely proven to be effective in distinguishing mangrove forest covers, even at the species level (Portengen. 2017). However, UAVs have more flexibility to record vegetation as they offer much higher spatial resolution (e.g. 0.13 m at ground level). UAV data enables detection of vegetation at low density areas and precise distinction between water, vegetation, and barren cover on the ground. It can also help to distinguish mangrove species and other vegetation types, integrating expert knowledge. Nevertheless, its advantage gradually reduces as the spatial extent of the study area increases. Thus, while Sentinel-2 data provides general characteristics of vegetation in extensive areas without the need of being physically present, UAV data is able to detect localized conditions, spatially in areas that are very heterogeneous. The physical presence needed when collecting data via UAV provides access to specific data for each site in the field, such as slopes, plant population densities, species presence, etc.

Thus, UAV data was used as an additional way to check how accurately the model performed over the study area. Although the classification results from Sentinel-2 data will be much coarser than the images provided by a drone, it is a useful way to qualitatively evaluate the accuracy of the results. The three UAV images acquired in 2019, provided by a local expert, were used to make a qualitative comparison with the classification results. The orthophoto mosaics of the drone images and the classification results were overlaid, and their level of coincidence is shown in Figure 27. Overall, the classification results from Sentinel-2 satellite imagery are considered to be reliable in classifying mangrove cover.

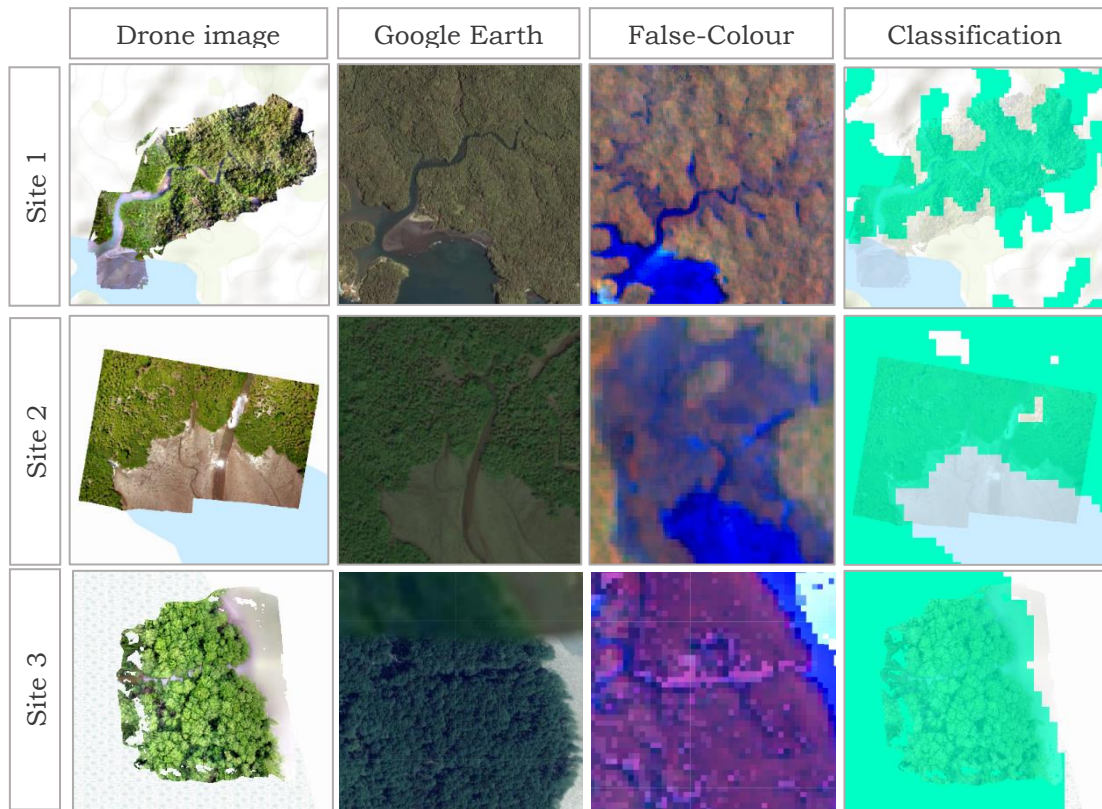


**Figure 27** Visual comparison between UAV orthophoto mosaics and the mangrove classification results

The scripts used for performing the classification can be accessed through this link to the GEE repository: [https://code.earthengine.google.com/?accept\\_repo=users/sgoros/AAA](https://code.earthengine.google.com/?accept_repo=users/sgoros/AAA)

## 6 VISUALIZATION

The following chapter briefly describes the methods, data and software used for the final objective of this study, which was the creation of a simple web-map for presenting the Colombian pacific coast mangrove forest classification outputs.

### 6.1 Geovisualization

Although a greater number of publications focus on data distribution and processing rather than visualization (Ruzicka et al., 2017), results of any spatial analysis cannot be interpreted and discussed without visualizing the data (Nétek et al. 2019). As new sensors and applications have been developed, there has been parallel development not only of spatial data processing tools and methods for extracting information, but also of tools for presenting such information.

Geovisualization, which is short for “Geographic Visualization“, can be defined as modern form of cartography in which the map is not only a representation, but rather a model for geospatial-oriented scientific visualization (Huisman & de By, 2009). It refers to tools and methods that support spatial data analysis and communication, and therefore are crucial for data exploration and decision-making processes. In the Remote Sensing field, geovisualization techniques are applied to integrate different analysis and applications and to extract and present the information that is useful or meaningful for a specific application (Masini. 2019). Remote sensing images were used throughout this study for information extraction of mangrove distributions, and the resulting products from processing such images can be presented through a variety of cartographical methods and visualization approaches. One of which is though web maps.

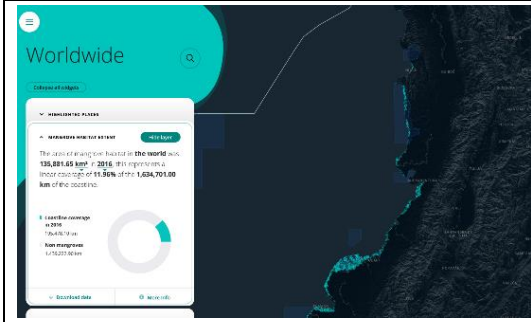
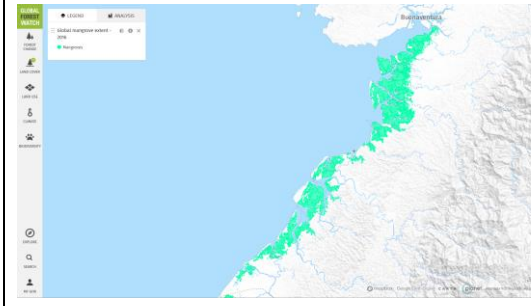
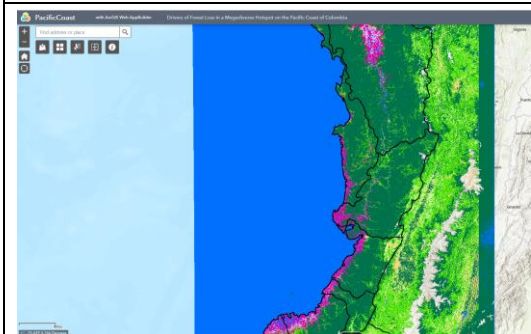
The first part if the thesis involved the extraction of information on mangrove distribution from Sentinel satellite data, performed using the Google Earth Engine, through its JavaScript API. A practical and fast option for visualizing the information is to make use of the User Interface API, providing a set of widgets, which gives you the possibility of publishing the results using the GEE Apps service. This option was explored to present the resulting layers of the classification. GEE Apps are sharable and dynamic user interfaces used for generating and visualizing GEE outputs (GEE, 2020). The published apps can be accessed by anyone using the application-specific URL, without the need of a GEE account. Thus, GEE’s JavaScript API offers a convenient solution to visualize the generated information as it is being processed, reducing the need for downloading, storing, and managing such large amounts of data once it is done. This option was explored using the client-side user interface (UI) `ui.SplitPanel` widget, which was useful for comparing the classification layers of different years for the same area (Cauca mangroves in 2017 and 2020).

Alternatively, the possibility of presenting the results in a custom web map application, using a solution outside of the GEE platform, was further evaluated. The aim was to find an appropriate solution to implement a simple web map for presenting the overall results from the analysis of the Colombian Pacific coast mangrove forests.



In the fields of natural resource monitoring and conservation, web map applications are increasingly being used to effectively convey spatial-related information. A few interesting web maps applications and tools involving the visualization of mangrove distribution data were explored. The maps and a short description are included in Table 15.

**Table 15** Reference mangrove web map applications

	<p><b>Global Mangrove Watch</b> (GMW) is an online platform that provides the remote sensing data and tools for monitoring mangroves necessary for this. It gives universal access to near real-time information on where and what changes there are to mangroves across the world and highlights why they are valuable. Web map link: <a href="http://www.globalmangrovetwatch.org">www.globalmangrovetwatch.org</a></p>
	<p><b>Global Forest Watch</b> (GFW) is an open-source web application made to help monitor mangrove forests globally, in near real-time. The application is an initiative developed by WRI, partnering with Google, USAID, the University of Maryland (UMD), Esri, Vizzuality, as well as with public, academic, non-profit and private organizations. Web map link: <a href="http://www.globalforestwatch.org">www.globalforestwatch.org</a></p>
	<p><b>PacificCoast</b> is a web map developed to showcase the classification outputs of Anaya et al. (2020). Operational layers include derived mangrove forest covers in the Colombian pacific coast, and ancillary data. Web map link: <a href="https://geomatica.udem.edu.co/flexviewers/PACIFICCO/index.html">https://geomatica.udem.edu.co/flexviewers/PACIFICCO/index.html</a></p>

## 6.2 Web mapping tools and libraries

As digital transformation relocates from desktop platforms to the internet environment, new technologies in the field of web cartography and WebGIS (Web Geographic Information Systems) are rapidly emerging. This together with access to large volumes of data has enabled the production of high-quality maps with high-quality information (Eicher, 2018). Web maps deal with the map product, its technical solution and visualization. They are an extremely efficient and far-reaching tools, for sharing information. These traits have led them to far surpass traditional (analog) maps in terms of accessibility and popularity (Nétek, 2020). Consequently, at present, a considerable amount of technologies for web mapping are available, providing a wide range of options.

Currently most web mapping libraries are based on JavaScript Technology (Nétek et al. 2019; Nétek, 2016). JavaScript is one of the most popular programming languages for web pages in general, but also within the web-mapping community in their ongoing quest for developing code-free graphical interfaces that allow making sophisticated web maps (Dorman, 2020). In their study, Nétek et al. (2019) compare popular JavaScript mapping libraries such as Leaflet and OpenLayers to analyze web-based visualization possibilities in the current times of Big data. OpenLayers and Leaflet are well-known open-source mapping libraries based on JavaScript. Leaflet for instance, is leading in terms of developing mobile-friendly interactive maps. It works efficiently across platforms, is easy to use and well documented, and has a wide range of feature options that can be used to create from simple web maps to very complex web mapping applications (Pánek and Burian, 2020). OpenLayers is a more complex and heavier solution compared to Leaflet. It is commonly used for dynamic web maps and is well suited for the display of map tiles and vector data from any source (Pánek and Burina, 2020). Mapbox is another popularly used library that allows the users to create custom designed maps and integrate them into applications via API's. Many websites and applications use this solution for advanced customization. However, it has a steep learning curve and it is only free up to a certain limit (freemium), based on page requests and map views.

The advantage of these libraries is that they offer high possibilities of interactivity, adjustable dynamics, many options to choose from in terms of functionality and features, which are generally well documented. The disadvantage can be related to their complexity. They require the user to have coding knowledge and, depending on the complexity of the web application required, the development process can get considerably challenging. Moreover, there is the server issue. In order to share a web map on the web, a server is required.

A solution to this is to resort to cloud-based platforms that provide their own server for storing and publishing the information. Cloud solutions are becoming ever more popular as they develop their interactivity and customization options. Examples of this type of solution are QGIS cloud, Mapbox, or Esri's ArcGIS Online. The ArcGIS online platform requires that the user has an account. Although the public account is free it has limitations in terms of limited amount of feature upload, limited formats, and storage, among others. The Enterprise login, available for institutions who have paid for it (e.g. Palacký University and Salzburg University) is less restricted. Maps and data can be stored in the cloud and are accessible from anywhere. Moreover, local data can be uploaded in different formats and online data can be easily linked (Pánek and Burian, 2020). Additionally, this solution allows making online maps without a single line of code. In addition to these solutions, several platforms are providing intuitive interactive interfaces for creating and publishing web maps and web mapping applications, such as Mapbox Studio or Esri's Web App Builder.

Considering the simplicity of the web-map interface required, and factors including the type of datasets to showcase, the access provided by the university's Esri Enterprise account, the connection between ArcGIS Pro, ArcGIS Online and the Web AppBuilder platforms, and the access to ArcGIS Server, among others, provided enough reasons to

support the choice of ArcGIS Online as an appropriate alternative solution for developing the final mangrove forest cover web map application.

### 6.3 Web map creation

Web mapping involves a complex process, which begins with the initial idea. It has been referred to as the “think before you draw” (Voženílek, 2009) or in this case the “think before you click” phase (Nétek, 2020). It requires the mapmaker to reflect on the purpose of the map, the use of the final outputs, which includes the choices of data sources and libraries. Once the map has been developed the map-use from the user’s point of view should be tested and reflections on cartographic and web rules should be made. The field of user research and testing is highly complex. User testing is performed considering the user requirements, thus, analyzing the map use from the viewpoint of prospective end users. It is an essential part of map production. In the scope of this study, however, having not fully identified the specific end user and due to time constraints, user testing was not performed. It was considered, nonetheless, as an essential next step to take in future developments and at the very least should be mentioned. The final phase, which involves publishing the product, considers how the map is disseminated over the network.

Within the scope of this study, the implementation of the web map application was done following the procedure in Figure 28 The process involved the use of ESRI’s ArcGIS pro, ArcGIS online and Web App Builder. The layer preparation (generalization and attribute information) was performed in ArcGIS Pro. The layers were then imported to ArcGIS Online for styling and sharing with ESRI Web AppBuilder for the final web map application customization and publication.

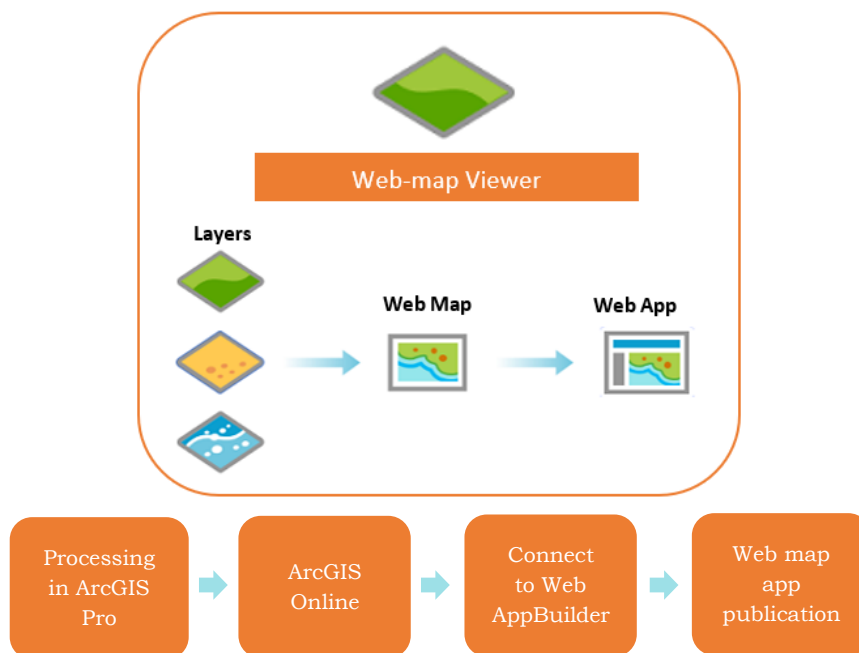


**Figure 28** Workflow

### 6.3.1 User interface layout and input data

Web maps can be used to inform a wide audience on the web by displaying geographical information, but before making any decision, it is important to take into consideration what data will be included, what format, how to categorize data, how to keep it consistent, etc. The information that the map carries must well represented in order to be well communicated. The same as with traditional maps, when creating a map interface layout there are design principles to consider. Among these are legibility, hierarchical organization, visual contrast, and balance. Without these, the map may not be able to communicate effectively.

Sketching the interface layout of the web-map and defining the data to be included, can also motivate the decision on the library solution to choose. As described before, different web mapping tools offer different possibilities and some can be more appropriate depending on the purpose of the map, its content, the needs and skills of the mapmaker, and the resources available. The web map solutions should always be selected for a reason, and the clearer the planning and thinking process, the better choices can be made. The “thinking before drawing”, in this sense, can be followed by the “drawing before implementing” phase, which also involves considering the user the map is intended for, the data to include, the preferred layout, the interactivity, functionality and complexity required, among others.

Therefore, in this study the map sketching process did not only influence the selection of the web map library solution, but also supported the decisions taken in terms of the layers to be included, the structure of the map and the pursued design in general. The sketch (Figure 29) helped to generally identify the layers and interactivity pursued. At the same time, it motivated thoughts on potential colour templates and the options for displaying the content of the layers (pop-ups, attributes, descriptions etc).

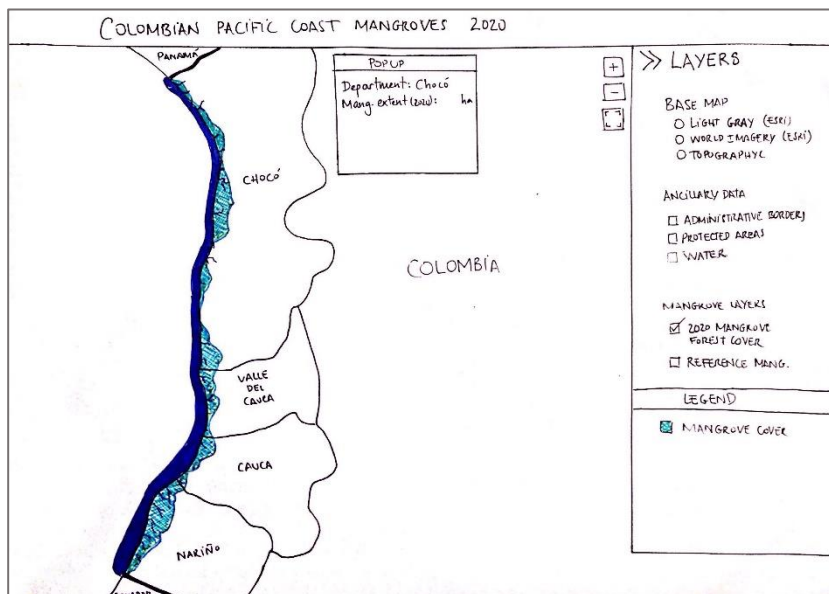


Figure 29 Web map sketch

The objective was to create a simple web-map for displaying the classification outputs obtained from the analysis part of the thesis. In terms of content, a web map in its most basic form will contain a basemap, some operational layers, navigational tools and an initial extent. The basemap layer helps provide the geographical context and frame of reference for the operational layers. The operational layers are the main focus and are displayed on top of the basemap layer. The layers to be included in the web map are listed in Table 16

**Table 16** Reference mangrove web map applications

Layer	Coverage	Type	Format	Source
Mangrove cover 2020	Colombian Pacific coast	Raster /discrete	shapefile	Self-generated
Protected areas	Colombia	Vector (polygon)	shapefile	Esri open data
Sentinel-2 composite 2020 (false-color)	Colombian Pacific coast	Raster (false.color composite)	Raster tiles	Self-generated
Water mask (S1 + S2)	Colombian Pacific coast	Vector (polygon)	shapefile	Self-generated
Drone image locations	Site	Vector (points)	GeoTIFF	Gustavo Castellano Galindos (WWF, Germany)

### 6.3.2 Data processing in ArcGIS Pro

After the classification process, the mangrove forest cover outputs were exported from GEE in raster format, and imported into ArcGIS Pro, where they were further processed.

#### Vector layers

The mangrove cover and water layers were the only outputs converted into vector format. Vector layers allow the retrieval of attribute information when clicking on the layers (e.g. pop-ups), and symbology can be easily changed. However, the layer loading speed is largely affected by the complexity of the geometries of the displayed elements. Smoothing is a way to reduce this complexity, but at the expense of resolution, and therefore it can be a challenge to decide the level of generalization that one should apply. A way to approach this is to try different levels of generalization and chose the level that preserved the quality and accuracy of the information as much as possible, while still improving loading speeds. Administrative borders included for the pacific coast departments were also generalized. Once all the vector layers were ready, they were exported as shapefiles and then embedded into a zip folder, following recommendations for uploading to ArcGIS Online.

#### Raster Layers

The Sentinel-2 false-colour composites, were downloaded and converted to raster tiles using MapTiler. Raster tiles are made up of smaller manageable areas that together make up for an image, which are sorted in a database, commonly by zoom level. Raster tiles are fast to transmit, they offer good performance, and can be interpreted by most common mapping software applications (ArcGIS Online, 2020). MapTiler, is a service that allows a user to create map tiles from his/her own data and it is very popularly used. The software can be downloaded as a desktop application or as a cloud service, and used for free, but with some limitations. The free version of MapTiler (which was used in this study), only permits a maximum raster size of 10,000 x 10,000 pixels. Therefore, one must make sure that the raster files do not exceed the limit. In case that the files exceed the extent, it is necessary to export the image in smaller sections.

### **6.3.3 Map styling in ArcGIS Online**

The possibility of styling maps interactively through ArcGIS Online is very practical. ArcGIS Online stores and hosts a set of existing web apps which can be easily customized and shared over the server. Alternatively, it offers the possibility of downloading the code locally and to host and customize the web app on your own. ArcGIS Online is connected to the Web App Builder (WAB) tool, which is very intuitive and can be used to create both 2D and 3D web applications. Several full-featured HTML apps are available for customization (ESRI, 2020), and any changes or additions applied can be seen in the application simultaneously. The WAB allows creating HTML/JavaScript applications that run on any device, access ready-to-use widgets that can be embedded in other applications.

#### **Symbology**

The symbology and scalability of each of the layers was edited in ArcGIS online. Symbolization can help communicate the meaning of the web map to the users. The ability to change symbology is one of the main advantages of vector tiles. Symbolization for points, lines, and polygons should be simple and easily understood. Using ArcGIS Pro it is possible to set up complex symbology, but symbols may be downgraded when shared as part of a web map in ArcGIS online. Therefore, symbology configuration was finalized in ArcGIS Online. The mangrove layer was symbolized with a bright blue colour, inspired by the mangrove map by Global Mangrove Watch web map application. To improve the contrast with the background and highlight the mangrove layer, the dark-grey basemap provided better results among the options. Therefore, it was chosen as the active basemap when the application is opened. The water layer was set to a dark blue, which contrasted well with the mangrove layer and the background layer. Points used to indicate the sites from which the UAV images were taken, were symbolized with location markers.

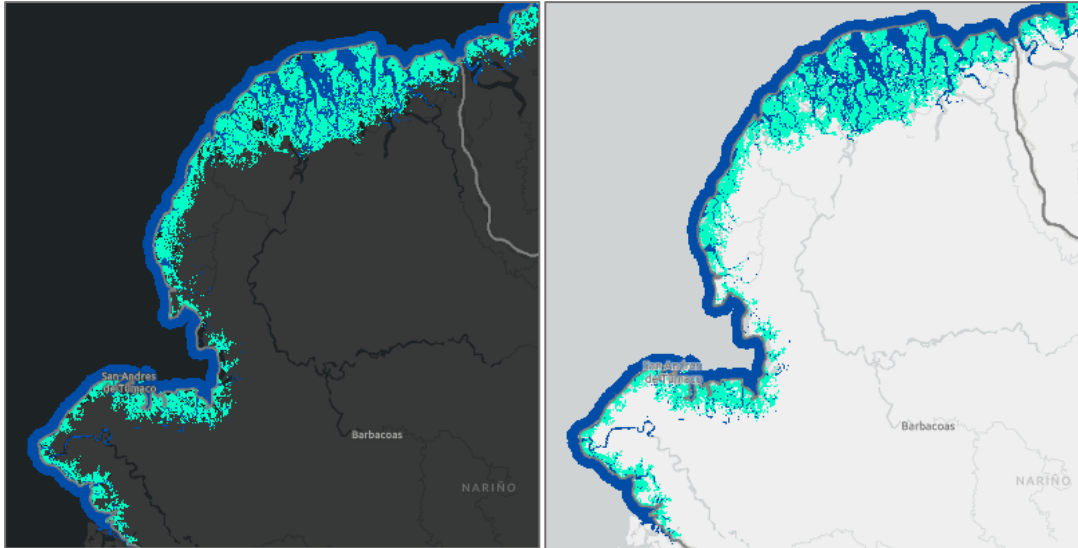


**Figure 30** Screenshot of the looks of the dark-gray and light-gray basemaps (Google basemaps) with the operational layers

### Pop-ups

The mangrove layer pop-ups were configured to show specific information, by modifying fields, formatting data, and adding charts. For instance, a pie chart was included in the administrative layer for indicating the portion of mangroves that occupy in each department against the entire mangrove extent of the region (Fig 31). A bar chart was also included in the mangrove layer pop-up information for displaying the estimates that had been done by other studies, for different years.

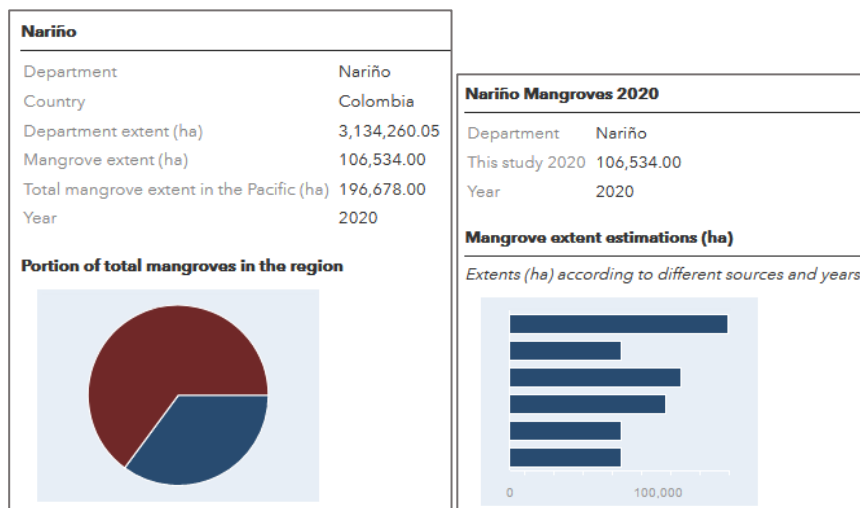


**Figure 31** Pop-ups from the department layer (left) and the mangrove layer (right)

### 6.3.4 Publishing the web map

When saved, the web map is registered in the content of the user of the organization to which it belongs. The map can be published as a web map application using the

Configurable Application, the Web AppBuilder of the Operations Dashboard option. In this case the Web AppBuilder was used. The template (Foldable theme) was selected, and a few modifications were made, including the addition of widgets. Finally the „Mangrove Forests of the Colombian Pacific Coast 2020“ web map application was published.

## 6.4 Results

In order to represent the results in a more simple and generalized way, a simple custom-made ArcGIS Web App was created with the use of ESRI WebAppBuilder.

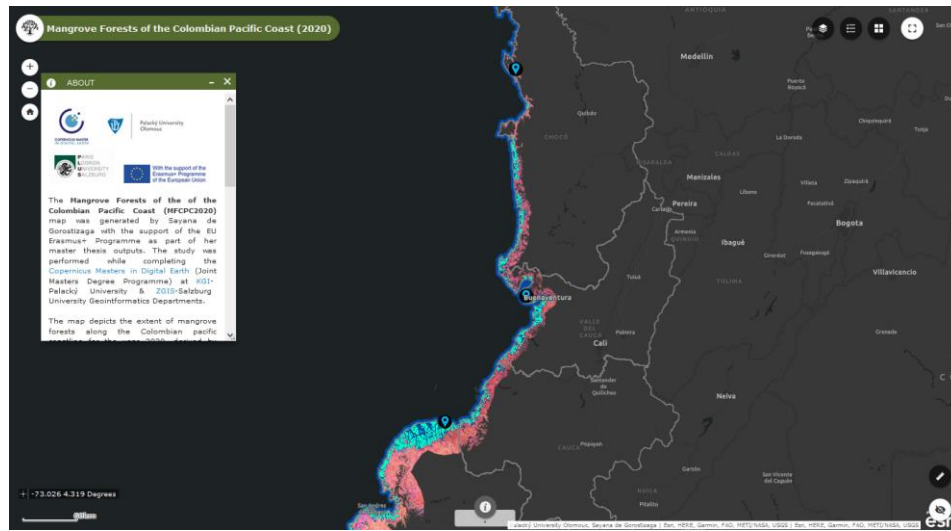


**Figure 32** Pop-ups from the department layer (left) and the mangrove layer (right)

The layers were processed in which they were examined, adjusted to a defined buffer zone, and generalized. This layer processing step was performed in ArcGIS Pro. The layers were then transferred into the ArcGIS Online platform in order to properly symbolize them and set up the attribute information that would be displayed (pop-ups). The web map was then connected to the Web AppBuilder for customizing the user interface and publishing the web map application. The final web map application contains the generalized mangrove classification layers the year 2020 of the entire Colombian Pacific coast. The application is open to the public and presents a simple user interface for visualizing mangrove extents and distribution across the Colombian Pacific coast.

### **Web map application link:**

<https://zgis.maps.arcgis.com/apps/webappviewer/index.html?id=9c47409317d94cfc96002d8519f66622>



## 7 DISCUSSION

### **Does the combination of Sentinel-2 optical with Sentinel-1 radar data improve classification accuracies?**

Previous research has proven that radar and optical data combined improved land cover classification (Shapiro et al., 2018; Zhen et al. 2018; Portengen, 2017; Fatoyonibo et al 2008). However, the results of this study, show that models using Sentinel-2 (S2) data only, perform as well as the model combined with Sentinel-1 (S1) data for annual composites. Using the S1-only model underperformed compared to using S2-only model for the Cauca department, however it still performed quite well with an accuracy of 90%. However, Sentinel-1 data was used in all models for masking out water, as it provided improved results, compared to water masking using Sentinel-2 data. The fact that masking out water largely reduces a common source of misclassification (water as mangrove cover), means that Sentinel-1 does improve the classification accuracy.

The S1-only model was able to identify mangrove cover but presented a higher number of misclassifications visible within the non-mangrove areas which could be caused by textural similarities with other types of vegetation. The S1 model overestimates mangrove cover, which could also be influenced by high surface roughness producing similar signals for different types of trees and shrubs. Moreover, the S1-only model could be less accurate due to errors caused by incidence angle variation, speckle, moisture content and geolocation accuracy (Borges et al. 2020). Zhang et al. (2019) showed that S1 data overestimated woody vegetation presence in different parts of Africa.

The S2 model based on the masked median and the S2 model based on the greenest pixel, performed almost equally well, with overall accuracies above 94%. The greenest pixel model was used for all the departments in the Colombian Pacific region, obtaining accuracies between 92% and 97%. Only two classes (mangrove and non-mangrove) were used in the models, which might partly explain the overall very high accuracy results. Another possibility would be high overlap of training and validation points, but that was checked with detail. Thus, a more thorough evaluation of possible sources of errors causing high accuracies should be made in order ensure the trustworthiness of the results.

To produce the greenest pixel composite requires much less effort than to produce the median masked composite or the Sentinel-1 composite. By using a full year collection of data, it is possible to obtain a cloud-free image, good enough to perform effectively and as well as a masked image. The model may not perform as well, if applying it seasonally, since the number of images is considerably reduced. However, within the scope of this study, the data over the period of one year was used and the seasonal influence on the accuracies was not further explored. The results obtained can be related to the results of Symeonakis et al (2018) and Borges et al (2020), who found that the multi-sensor approach was only marginally beneficial (around 1% approx.), and that if multi-season data is available, combining more than one sensor might be unnecessary and even counterproductive for specific land cover classes. It is possible to conclude that Sentinel-

1 did not bring much improvement to the performance of the classification model, however it did improve the classification outcomes by effectively masking out water. Therefore, the combination of Sentinel-1 and Sentinel-2 did improve the classification accuracies.

### **Is the model transferable to other locations and years?**

The classification model applied to each department performed well, as indicated by the resulting accuracies (between 92 and 97 percent). Although the accuracies for each of the departments were high, it should not be the only factor in deciding whether the model performed well or not. In the composite creation phase a visual evaluation of the quality of the images was performed to make sure of their quality before they were submitted to classification. In some cases, the greenest pixel method may not suffice and applying a mask for clouds and shadows will be necessary. Moreover, for identifying and defining spectral reflectance behaviours for different landcover types (e.g. water) the greenest pixel composites will not be useful. For cases in which cloud and shadow presence remains high even after applying cloud and shadow masks, the Sentinel-1 model promises an adequate performance, considering the accuracy results. In this study, however, the Sentinel-2 greenest pixel model performed well enough for detecting mangrove cover and estimating extents over the entire Colombian Pacific coast. The mangrove forest extent estimates showed higher values than those determined by the most global-scale studies with remote sensing (Hamilton and Casey 2016; Giri et al 2011), which are all much lower than national-scale studies (IGAC, 1966; Zambrano-Escamilla and Rubiano-Rubiano 1996; Orjuela et al, 2009; Invemar, 2015) (Table 17). However, the fact that it estimated similar values to the national-scale study estimates is also a good sign of the model's performance. The closest estimates were those reported by Orjuela et al. (2009) and Invemar (2015), which is a coastal research institute leading the mangrove monitoring program in the country. It is also important to acknowledge that the mentioned studies have all used different methods, and lower resolutions, which could mean that smaller patches of mangroves were not detected, especially for the case of global datasets. Thus, these patches are more likely to be detected using Sentinel-2 satellite data and accounted for in the estimations.

**Table 17** Reference mangrove extent estimates by department

<b>Province</b>	<b>IGAC (1966) 1966 (ha)</b>	<b>Zambrano-Escamilla and Rubiano-Rubiano (1996) (ha) 1992</b>	<b>Orjuela et al., 2009</b>	<b>Giri et al. (2011) 2000 (ha)</b>	<b>SIGMA (INVEMAR, 2015) 2014 (ha)</b>	<b>Hamilton and Casey (2016) 2014 (ha)</b>	<b>GMW 2016 v2 (ha)</b>	<b>Current study (2020)</b>
Chocó	79,918	64,750	64,750	22,368	41,331	18,418	24,900	42,651
Valle del Cauca	48,396	41,961	31,374	30,155	31,478	21,848	20,288	29,688
Cauca	59,648	36,276	19,703	16,403	19,125	15,571	11,362	17,805
Nariño	172,083	149,735	117,576	76,382	117,468	76,262	105,089	106,534
Total	360,083	292,724	233,403	132,325	209,402	132,099	161,639	196,678

Additionally, the model run over a different year (2017). The accuracy values remained high with an overall accuracy of 97%. These results might confine the model the potential of being used for change detection, which was tested. The difference from the 2017 and 2020 extents was calculated and resulted in a change of 1,435 ha. The significance of these result, however, need further evaluation. An assessment of the quality and interpretation should be made, which was not in the scope of this study. These results, however, indicate that the model could potentially be used for estimating mangrove extent and distribution over different years.

### **What is an appropriate solution for visualizing the classification outputs?**

The use of Google Earth Engine Apps service with support of the User Interface API can provide practical and easy solution since it allows the entire processing and visualization steps to be taken in the same platform without the need of downloading the data. Also, due to the fast rendering of datasets, resulting from GEE's processing power, the need for generalizing the data is less apparent. This option requires less time spent on data preparation as opposed to using other web mapping solutions which require the data to be reduced, generalized, or transformed to other formats. Moreover, GEE's data catalogue makes it useful for combining the data with additional sources of information (e.g. CHIRPS precipitation data) right on the spot. As previously mentioned, ancillary data is important to provide a better understanding of the outputs. Nonetheless, the functionality provided by solutions like that of GEE is reduced compared to tools that have been specifically developed for the purpose of map creation, rather than data processing and analysis. Also, customization in GEE is limited, and for instance although it is possible to somewhat customize the base map, it is not possible to add external basemaps from other platforms other than Google. Although Google basemaps are a preferred choice for many, it may not be favoured in all cases. The simple GEE web map apps were made taking advantage of the convenient services connected to the platform in which the data was processed. It was a quick solution which may be enough in some cases.

Taking advantage of the university's Enterprise licence, the possibility of creating a web map application using ArcGIS Online was evaluated. The advantage that ArcGIS provided over the GEE Apps solution was it was easier to manipulate and process the data to depict the information I was seeking to display. The process of making a map in ArcGIS Online is intuitive and allows for much more styling of the layers and better customization of overall map application, compared to the GEE solution. It provided a greater range for choice. ArcGIS Online is connected to ArcGIS Pro, where it is easier to prepare the data. With ArcGIS pro raster layers can be easily transformed to vector, and vector opens new possibilities of symbolization, generalization and addition of information. The vector format was important to provide interactivity in the final web map application, as the user can click on the layers and obtain additional information from the pop-ups. Using ArcGIS Online, maps can be created with just a few steps and are easy embedded in a web map application though the Web AppBuilder. Compared to the GEE-based web apps, with the ArcGIS online solution the communication capacity of the map was enhanced.

ArcGIS Online and the Web AppBuilder covered what was needed for producing the expected web map application within this study's scope. Nonetheless, for future

development, user testing and a deeper exploration of other solutions, preferably open-source libraries (e.g. Leaflet, OpenLayers, etc.), should be made in order to fully determine the solution choice and performance of the created web map application.

## 8 CONCLUSION

Remote sensing represents an essential instrument to monitor mangrove forest distributions and their dynamics all over the world. Technological advancements in cloud-computing services such as the Google Earth Engine (GEE), are helping reduce the practical limitations concerning processing power and data availability. Moreover, with the growing availability of free high-resolution imagery, like the optical Sentinel-2 and radar Sentinel-1 satellite imagery, the potential for studying land cover distribution and dynamics has largely expanded.

Studies around the globe mapping mangroves and other landcover types have demonstrated that in situations where optical data may be limited (e.g. due to dense cloud cover) the use of radar data alone or in combination with optical data can provide considerable advantages over using the optical only (Zhen et al., 2018, Shapiro et al. 2018). The Colombian pacific coast, being a region with extensive mangrove forest cover that has not been consistently mapped, and being one of the cloudiest spots in the world, was considered a good testing spot for the above-mentioned approaches. The study made use of data acquired by the Copernicus Sentinel-1 (radar) and Sentinel-2 (optical) missions and combined them with the capabilities of GEE, together with state-of-the-art classification approaches, to derive mangrove forest distributions across the Colombian Pacific coastline for the year 2020.

The results revealed that all models applied (accuracies between 90% and 97%) were viable options for classifying mangrove cover. However, contrary to what previous researchers have shown, the combination of optical and radar data did not significantly improve the accuracy results (less than 1% accuracy improvement). However, the radar data did offer an improvement for masking out water and therefore did in fact allow for higher accuracies. The model that required less processing effort integrated a composite made applying a quality mosaic method, based on NDVI values. This model in terms of accuracy performed as well as the model integrating a masked median composite, and insignificantly less than the combined model (less than 1% over). All models performed better than the one based on Sentinel-1 data. The greenest pixel model was therefore applied to the departments located along the Colombian Pacific Coast bearing high accuracies (92% to 97%). The mangrove cover distributions were mapped and their extents for the year 2020 was derived. Consequently, a mangrove forest layer was generated for each of the four departments in the study area (Chocó, Valle del Cauca, Cauca, and Nariño).

Considering the results, it was possible to determine that if annual data is available, the effort required for obtaining a cloud free image may be reduced by applying the greenest pixel method. Moreover, the benefits of combine multi-sensor data for deriving an optimal classification model can be outweighed by the efforts required to process such data. The results demonstrated the application and value of the approach that was used to uncover the distribution of mangrove forests in a tropical region, where cloud-prevalence can generate limitations to using optical imagery. Thus, optical data alone may suffice for annual mangrove classification even in the cloudiest of regions. The resulting classification approach could be used to map mangroves at regional and national-scale and help fill-in information gaps for better mangrove ecosystem understanding,

management and protection. The final outputs were embedded in a web map application in order to provide a more flexible, interactive and detailed look into the mangrove forest cover estimates with regard to departments.

Overall, this study contributes to the application of the GEE cloud-computing platform and Copernicus Sentinel-1 and Sentinel-2 satellite data, and their potential for monitoring and mapping mangrove forest cover. It also acknowledges the importance of considering ways to better visualize and present the results considering the map purpose, the data and the user requirements.

Several recommendations could be made from this study. Mangrove cover estimations using different sensors should be made to compare performances. The benefits and limitations of combining different optical satellite data (e.g. Landsat and Sentinel) should be explored in the region. An additional source of data could fill in gaps and provide enough images for exploring the influence of tides and seasons. Seasonality and tide calibration were explored, but not developed in this study due to insufficient images from Sentinel-2 alone. The application of tide calibration, for instance, has been done by other studies (Yancho et al 2020) and merits exploration in the context of the Colombian Pacific. Moreover, it would be beneficial to assess outputs and performances of different optical satellite data using the workflow applied in this study. The complexity of processing Sentinel-1 data should motivate further exploration to discover its potential. Parameters like the Radar Vegetation Index (RVI) may bring a valuable input from its integration. Access to more field data will improve the confidence in the results. Finally, analysis of change detection will help identify forest degradation hotspots, which will provide a valuable input into management and conservation initiatives.

## REFERENCES

Álvarez-León, Ricardo. (2019). Management of Mangrove Ecosystems: Republic of Colombia, South America. 1-023.

Alvin B. Baloloy, Ariel C. Blanco, Raymund Rhommel C. Sta. Ana, Kazuo Nadaoka, (2020) Development and application of a new mangrove vegetation index (MVI) for rapid and accurate mangrove mapping, ISPRS Journal of Photogrammetry and Remote Sensing, Volume 166, Pages 95-117, ISSN 0924-2716, <https://doi.org/10.1016/j.isprsjprs.2020.06.001>.

Ananto, Putri, Hadi, Hanum, Wiryawan, Prabaswara, Arjasakusuma, (2019); "Performance of various speckle filter methods in modelling forest aboveground biomass using Sentinel-1 data: case study of Barru Regency, South Sulawesi," Proc. SPIE 11311, Sixth Geoinformation Science Symposium, 113110P; <https://doi.org/10.1117/12.2549036>

Anaya, Jesús A.; Gutiérrez-Vélez, Víctor H.; Pacheco-Pascagaza, Ana M.; Palomino-Ángel, Sebastián; Han, Natasha; Balzter, Heiko. (2020). "Drivers of Forest Loss in a Megadiverse Hotspot on the Pacific Coast of Colombia" Remote Sens. 12, no. 8: 1235. <https://doi.org/10.3390/rs12081235>

Belgiu, Mariana & Drăguț, Lucian. (2016). Random forest in remote sensing: A review of applications and future directions. ISPRS Journal of Photogrammetry and Remote Sensing. 114. 24-31. [10.1016/j.isprsjprs.2016.01.011](https://doi.org/10.1016/j.isprsjprs.2016.01.011).

Bunting P., Rosenqvist A., Lucas R., Rebelo L-M., Hilarides L., Thomas N., Hardy A., Itoh T., Shimada M. and Finlayson C.M. (2018). The Global Mangrove Watch – a New 2010 Global Baseline of Mangrove Extent. Remote Sensing 10(10): 1669. doi: [10.3390/rs1010669](https://doi.org/10.3390/rs1010669).

Blanco-Libreros, J. F. (2016). Cambios globales en los manglares del golfo de Urabá (Colombia): entre la cambiante línea costera y la frontera agropecuaria en expansión. Actualidades Biológicas, 38(104), 53-70 <https://doi.org/10.17533/>

Blanco-Libreros, J.F., Estrada-Urrea, E.A., Ortiz-Acevedo, L., Urrego, L.E. (2012). Ecosystem-wide impacts of deforestation in mangroves: The Urabá Gulf (Colombian Caribbean): Case study. ISRN Ecology. 2012: 1-14.

Blum and Herr (2017) Mangrove restoration series. IUCN Global Forest and Climate Change Programme. Accessed in February 2021. <https://www.iucn.org/news/forests/201703/can-restoring-mangroves-help-achieve-sustainable-development-goals>

Borges, Joana & Higginbottom, Thomas & Symeonakis, Elias & Jones, Martin. (2020). Sentinel-1 and Sentinel-2 Data for Savannah Land Cover Mapping: Optimising the Combination of Sensors and Seasons. *Remote Sensing*. 10.3390/rs12233862.

Brisco, B. (2015) Mapping and monitoring surface water and wetlands with synthetic aperture radar. In *Remote Sensing of Wetlands: Applications and Advances*; Tiner, R., Lang, M., Klemas, V., Eds.; CRC Press: Boca Raton, FL, USA,

Cazals, C.; Rapinel, S.; Frison, P.-L.; Bonis, A.; Mercier, G.; Mallet, C.; Corgne, S.; Rudant, J.-P. (2016) Mapping and characterization of hydrological dynamics in a coastal marsh using high temporal resolution sentinel-1A images. *Remote Sens.* 8, 570.

Bangqian Chen, Xiangming Xiao, Xiangping Li, Lianghao Pan, Russell Doughty, Jun Ma, Jinwei Dong, Yuanwei Qin, Bin Zhao, Zhixiang Wu, Rui Sun, Guoyu Lan, Guishui Xie, Nicholas Clinton, Chandra Giri, (2017) A mangrove forest map of China in 2015: Analysis of time series Landsat 7/8 and Sentinel-1A imagery in Google Earth Engine cloud computing platform, *ISPRS Journal of Photogrammetry and Remote Sensing*, Volume 131, Pages 104-120, ISSN 0924-2716, <https://doi.org/10.1016/j.isprsjprs.2017.07.011>.

Clerici, N., Armenteras, D., Kareiva, P. et al. (2020) Deforestation in Colombian protected areas increased during post-conflict periods. *Sci Rep* 10, 4971 <https://doi.org/10.1038/s41598-020-61861-y>

R. Coluzzi, V. Imbrenda, M. Lanfredi, T. Simoniello (2018). A first assessment of the Sentinel-2 level 1C cloud mask product to support informed surface analyses. *Remote Sens. Environ.*, 217 pp. 426-443, 10.1016/j.rse.2018.08.009

Correa, I. D., & Morton, R. A. (2010). Caribbean coast of Colombia. In E. F. C. Bird (Ed.), *Encyclopaedia of the World's coastal landforms* (pp. 259-264). Springer.

Courty, L.G.; Soriano-Monzalvo, J.C.; Pedrozo-Acuña, A (2019) Evaluation of open-access global digital elevation models (AW3D30, SRTM, and ASTER) for flood modelling purposes. *J. Flood Risk Manag.* 12, 1-14.

de Sousa C, Fatoyinbo L, Neigh C, Boucka F, Angoue V, Larsen T (2020) Cloud-computing and machine learning in support of country-level land cover and ecosystem extent mapping in Liberia and Gabon. *PLoS ONE* 15(1): e0227438. <https://doi.org/10.1371/journal.pone.0227438>

Diniz, C.; Cortinhas, L.; Nerino, G.; Rodrigues, J.; Sadeck, L.; Adami, M.; Souza-Filho, P.W.M. (2019) Brazilian mangrove status: Three decades of satellite data analysis. *Remote Sens.* 11, 808.

Dorman, M. (2020). *Introduction to Web Mapping*. CRC Press. ISBN 9780367861186



Eicher, L. (2018). Development of a framework for designing a map style across several scales and its implementation (Master Thesis). Dresden University of Technology. Dresden. Source: Microsoft Word - Thesis\_Finalcocmp.docx (cartographymaster.eu)

Etter, Andres & Mcalpine, Clive & Phinn, Stuart & Pullar, David & Possingham, Hugh. (2006). Unplanned land clearing of Colombian rainforests: Spreading like disease?. *Landscape and Urban Planning*. 77. 240-254. 10.1016/j.landurbplan.2005.03.002.

European Space Agency. 2020 Sentinel-2 Products Specification Document. Thales Alenia Space. Disponible en: [https://sentinel.esa.int/documents/247904/349490/S2\\_MSI\\_Product\\_Specification.pdf](https://sentinel.esa.int/documents/247904/349490/S2_MSI_Product_Specification.pdf)

Fatoyinbo, T.E.; Simard, M.; Washington-Allen, R.A.; Shugart, H.H. (2008) Landscape-scale extent, height, biomass, and carbon estimation of Mozambique's mangrove forests with Landsat ETM+ and Shuttle Radar Topography Mission elevation data. *J. Geophys. Res. Biogeosci.*, 113, G02S06

Flores, Africa & Herndon, K. & Thapa, Rajesh & Cherrington, Emil. (2019). The SAR Handbook: Comprehensive Methodologies for Forest Monitoring and Biomass Estimation. 10.25966/nr2c-s697.

Fanco, L. (2007). Programa de áreas marinas y costeras protegidas del Caribe y Pacífico colombiano -bases para su desarrollo. Patrimonio Natural. Fondo para la Biodiversidad y Áreas Protegidas. Informe final de consultoría. Embajada del Reino de los países bajos. 94 p. [http://www.patrimonionatural.org.co/cargaarchivos/centroDoc/june\\_marie\\_mow\\_final.pdf](http://www.patrimonionatural.org.co/cargaarchivos/centroDoc/june_marie_mow_final.pdf). 23/08/2010

Funk, Chris, Pete Peterson, Martin Landsfeld, Diego Pedreros, James Verdin, Shraddhanand Shukla, Gregory Husak, James Rowland, Laura Harrison, Andrew Hoell & Joel Michaelsen. (2015) "The climate hazards infrared precipitation with stations—a new environmental record for monitoring extremes". *Scientific Data* 2, 150066. doi:10.1038/sdata.66 2015.

Giri C, Ochieng E, Tieszen LL, Zhu Z, Singh A, Loveland T, Masek J, Duke N (2011). Status and distribution of mangrove forests of the world using earth observation satellite data (version 1.4, updated by UNEP-WCMC). *Global Ecology and Biogeography* 20: 154-159. Paper DOI: 10.1111/j.1466-8238.2010.00584.x . Data DOI: <https://doi.org/10.34892/1411-w728>

Global Mangrove Watch, 2018. "Global Mangrove Extent (v2.0)." [www.globalmangrovetwatch.org](http://www.globalmangrovetwatch.org). Accessed through Global Forest Watch on 15/05/2021. [www.globalforestwatch.org](http://www.globalforestwatch.org).

Goldberg, L., Lagomasino, D., Thomas, N. and Fatoyinbo, T. (2020), Global declines in human-driven mangrove loss. *Glob Change Biol*. Accepted Author Manuscript. doi:10.1111/gcb.15275

Google Earth Engine.[online] Available from URL: <https://earthengine.google.com/>

Gupta, K.; Mukhopadhyay, A.; Giri, S.; Chanda, A.; Datta Majumdar, S.; Samanta, S.; Mitra, D.; Samal, R.N.; Pattnaik, A.K.; Hazra, S. (2018) An index for discrimination of mangroves from non-mangroves using LANDSAT 8 OLI imagery. *MethodsX* 5, 1129–1139. [CrossRef]

Gustavo A. Castellanos-Galindo, Lotta C. Kluger, Maria A. Camargo, Jaime Cantera, José Ernesto Mancera Pineda, Juan F. Blanco-Libreros, Matthias Wolff (2021). Mangrove research in Colombia: Temporal trends, geographical coverage and research gaps, *Estuarine, Coastal and Shelf Science*, Volume 248, 106799, ISSN 0272-7714, <https://doi.org/10.1016/j.ecss.2020.106799>.

Hamilton, S.E., Casey, D. (2016) Creation of a high spatio-temporal resolution global database of continuous mangrove forest cover for the 21st century (CGMFC-21). *Global Ecology and Biogeography*, 25(6), 729-738. <https://doi.org/10.1111/geb.12449>

Symeonakis, Elias; Higginbottom, Thomas P.; Petroulaki, Kyriaki; Rabe, Andreas. 2018. "Optimisation of Savannah Land Cover Characterisation with Optical and SAR Data" *Remote Sens.* 10, no. 4: 499. <https://doi.org/10.3390/rs10040499>

Hu, LuoJia & Xu, Nan & Liang, Jian & Li, Zhichao & Chen, Luzhen & Zhao, Feng. (2020). Advancing the Mapping of Mangrove Forests at National-Scale Using Sentinel-1 and Sentinel-2 Time-Series Data with Google Earth Engine: A Case Study in China. *Remote Sensing*. 10.3390/rs12193120.

Huisman & de By (eds.) (2009). *Principles of Geographic Information Systems – An introductory textbook*. ISSN 1567-5777 ITC Educational Textbook Series.

Invemar. (2010). *Sistema de Información Ambiental Marina de Colombia – SIAM. Red de vigilancia para la conservación y protección de las aguas marinas y costeras de Colombia – REDCAM*. <http://www.invemar.org.co/siam/redcam>

Invemar (2015) Instituto de Investigaciones Marinas y Costeras. Informe del estado de los ambientes258 y recursos marinos y costeros en Colombia: Año 2014. Serie de Publicaciones Periódicas259 No. 3. Santa Marta.

Jain, A.O.; Thaker, T.; Chaurasia, A.; Patel, P.; Singh, A.K. (2018) Vertical accuracy evaluation of SRTM-GL1, GDEM-V2, AW3D30 and CartoDEM-V3.1 of 30-m resolution with dual frequency GNSS for lower Tapi Basin India. *Geocarto Int.* 33, 1237–1256.

Kumar, Lalit; Mutanga, Onesimo. (2017). "Remote Sensing of Above-Ground Biomass" *Remote Sens.* 9, no. 9: 935. <https://doi.org/10.3390/rs9090935>

Kuenzer, C., Bluemel, A., Gebhardt, S., Quoc, T. V., Dech, S. (2011). Remote Sensing of Mangrove Ecosystems: A Review. *Remote Sensing*, 3(5), 878-928. <https://doi.org/10.3390/rs3050878>

MacEachren, A. M. and Kraak, M. J. (2001). Research challenges in geovisualization. *Cartography and Geographic Information Science (CaGIS)*, 28:3–12.

Mahdianpari, M., Salehi, B., Mohammadimanesh, F., Brisco, B., Mahdavi, S., Amani, M., Granger, J.E., (2018). Fisher Linear Discriminant Analysis of coherency matrix for wetland classification using PolSAR imagery. *Remote Sens. Environ.* 206, 300–317.

Mejia-Rentería, J.C., Castellanos-Galindo, G.A., Cantera-Kintz, J.R., Hamilton, S.E. (2018) A comparison of Colombian Pacific mangrove extent estimations: Implications for the conservation of a unique Neotropical tidal forest. *Estuarine, Coastal and Shelf Science*, 212(5), 233-240. <https://doi.org/10.1016/j.ecss.2018.07.020>

Minambiente - Ministerio de Ambiente y Desarrollo Sostenible de la República de Colombia (2017) Manglares: Los manglares de Colombia. Ministerio de Ambiente y Desarrollo Sostenible, Bogotá, <http://www.minambiente.gov.co/index.php/component/content/article?id=412:plantilla-a-bosques-biodiversidad-y-servicios-ecosistematicos-14>. Accessed 7 February 2020

Mondal, P., Trzaska, S., De Sherbinin, A. (2018). Landsat-derived estimates of mangrove extents in the Sierra Leone coastal landscape complex during 1990- 2016. *Sensors*, 18(1), 12. <https://doi.org/10.3390/s18010012>

Mondal, Pinki & Liu, Xue & Fatoyinbo, Lola & Lagomasino, David. (2019). Evaluating Combinations of Sentinel-2 Data and Machine-Learning Algorithms for Mangrove Mapping in West Africa. *Remote Sensing*. 11. 2928. [10.3390/rs11242928](https://doi.org/10.3390/rs11242928).

Muhsoni, F.F., Sambah, A.B., Mahmudi, M., Wiadnya, D.G.R. (2018). Comparison of Different Vegetation Indices for Assessing Mangrove Density Using Sentinel-2 Imagery. *International Journal of GEOMATE*, 14(45), 42-51. <https://doi.org/10.21660/2018.45.7177>

Nagy (2021) Obscured by Clouds: A Comparative Analysis of Cloud Removal Methods. *Medium*, <https://medium.com/project-canopy/obscured-by-clouds-a-comparative-analysis-of-cloud-removal-methods-b9b1c30c4e1f>

Netek, R (2006) Advanced GIS application for real-time crisis management support via internet platform. In *Proceedings of the SGEM2016 Conference*, Albena, Bulgaria, 28 June–6 ; Book 2; Volume 3, pp. 27–34; ISBN 978-619-7105-60-5; ISSN 1314-2704

Netek, R.; Brus, J.; Tomecka, O. Performance Testing on Marker Clustering and Heatmap Visualization Techniques: A Comparative Study on JavaScript Mapping Libraries. *ISPRS Int. J. Geo-Inf.* 2019, 8, 348.

Nétek, R. (2020). *Webová kartografie - specifika tvorby interaktivních map na webu*. Univerzita Palackého v Olomouci. 196 s. ISBN 978-80-244-5827-4.

Lang, M.; Bourgeau-Chavez, L.L.; Tiner, R.; Klemas, V. Chapter 5 (2015) *Advances in Remotely Sensed Data and Techniques for Wetland Mapping and Monitoring*. In *Remote Sensing of Wetlands: Applications and Advances*; CRC Press: Boca Raton, FL, USA,

Orjuela, A., C. Villamil, L. Perdomo, A. López y P. Sierra. (2009). Estado de conocimiento de los manglares. En: INVEMAR (Ed). *Informe del Estado de los Ambientes y Recursos Marinos y Costeros en Colombia: Año 2008*. Serie de Publicaciones Periódicas No. 8. Santa Marta. 89-108.

Otsu, N. A threshold selection method from gray-level histograms. *IEEE Trans. Syst. Man Cybern.* 1979, 9, 62–66. [Google Scholar] [CrossRef]

Perea-Ardila, M.A., Oviedo-Barrero, F., Leal-Villamil, J. (2019). Mangrove forest mapping through remote sensing imagery: study case for Buenaventura, Colombia. *Revista de Teledetección*, 53, 73-86. <https://doi.org/10.4995/raet.2019.11684>

Panek, Jiri & Burian, Jaroslav. (2020). Online Visualisation. 10.1007/978-3-030-26626-4\_10.

Pimple, U., Simo-netti, D., Sitthi, A., Pungkul, S., Leadpra-thom, K., Skupek, H., Som-ard, J., Gond, V. and Towprayoon, S. (2018) Google Earth Engine Based Three Decadal Landsat Imagery Analysis for Mapping of Mangrove Forests and Its Surroundings in the Trat Province of Thailand. *Journal of Computer and Communications*, 6, 247-264. <https://doi.org/10.4236/jcc.2018.61025>

Portengen, E.C. (2017). *Classifying Mangroves in Vietnam using Radar and Optical Satellite Remote Sensing*. Master thesis. Delft University of Technology. Delft.

Purwanto, Anang & Asriningrum, Wikanti. (2019). IDENTIFICATION OF MANGROVE FORESTS USING MULTISPECTRAL SATELLITE IMAGERIES. *International Journal of Remote Sensing and Earth Sciences (IJReSES)*. 16. 63. 10.30536/j.ijreses.2019.v16.a3097.

Ramsar Convention Secretariat. *The Fourth RAMSAR Strategic Plan 2016–2024*. Available online: <https://www.ramsar.org/the-ramsar-strategic-plan-2016--24> (accessed on 1 October 2020).

Reiche, Johannes & Verhoeven, Rob & Verbesselt, Jan & Hamunyela, Eliakim & Wielaard, Niels & Herold, Martin. (2018). Characterizing Tropical Forest Cover Loss Using Dense Sentinel-1 Data and Active Fire Alerts. *Remote Sensing*. 10. 10.3390/rs10050777.

Richards J.A. (1986) Supervised Classification Techniques. In: Remote Sensing Digital Image Analysis. Springer, Berlin, Heidelberg. [https://doi.org/10.1007/978-3-662-02462-1\\_8](https://doi.org/10.1007/978-3-662-02462-1_8)

Růžička, J.; Orčík, L.; Růžičková, K.; Kisztner, J. Processing LIDAR Data with Apache Hadoop. In The Rise of Big Spatial Data; Ivan, I., Singleton, A., Horák, J., Inspektor, T., Eds.; Springer: Cham, Switzerland, 2017; pp. 351–358; ISBN 978-3-319-45122-0; ISSN 1863-2246.

Sack, C. (2017). Web Mapping. The Geographic Information Science & Technology Body of Knowledge (4th Quarter 2017 Edition), John P. Wilson (ed.). DOI: 10.22224/gistbok/2017.4.11

Sánchez-Páez, H., Álvarez-León, R., Guevara-Mancera, O.A., Zamora-Guzmán, A., Rodríguez-Cruz, H., Bravo-Pazmiño, H.E. (1997b). Diagnóstico y zonificación preliminar de los manglares del Pacífico de Colombia, In: Sánchez-Páez, H. & Álvarez-León, R. (eds.) *Proy. PD 171 / 91 Rev. (F) Fase 1. Conservación y Manejo para el Uso Múltiple y el Desarrollo de los Manglares en Colombia*, MMA/OIMT. Santa Fe de Bogotá D. C. (Colombia), 343 p.

Schmitt, Michael & Hughes, Lloyd & Qiu, Chunping & Zhu, Xiao. (2019). Aggregating cloud-free Sentinel-2 images with Google Earth Engine. *ISPRS Annals of Photogrammetry, Remote Sensing and Spatial Information Sciences*. IV-2/W7. 145-152. 10.5194/isprs-annals-IV-2-W7-145-2019.

Schmitt, M., Hughes, L.H., Qiu, C., Zhu, X.X., (2019). SEN12MS – a curated dataset of georeferenced multi-spectral Sentinel-1/2 imagery for deep learning and data fusion. In: *ISPRS Annals of the Photogrammetry, Remote Sensing and Spatial Information Sciences*, volume IV-2/W7, pp. 153–160.

Senthilnath, J. & Handiru, Vikram & Rajendra, Ritwik & S N, Omkar & Mani, V & Diwakar, P.. (2013). Integration of speckle de-noising and image segmentation using Synthetic Aperture Radar image for flood extent extraction. *Journal of Earth System Science*. 122. 559-572. 10.1007/s12040-013-0305-z.

Shapiro, Aurelie & Trettin, Carl & Kuechly, Helga & Alavipanah, Sadroddin & Bandeira, Salomão. (2015). The Mangroves of the Zambezi Delta: Increase in Extent Observed via Satellite from 1994 to 2013. *Remote Sensing*. 7. 16504-16518. 10.3390/rs71215838.

Shapiro, Aurelie. (2018). Mozambique Mangrove Extent 1995-present. 10.13140/RG.2.2.18470.55367.

Simard, M., Fatoyinbo, L., Smetanka, C. et al. Mangrove canopy height globally related to precipitation, temperature and cyclone frequency. *Nature Geosci* 12, 40–45 (2019). <https://doi.org/10.1038/s41561-018-0279-1>

Sudmanns, Martin & Tiede, Dirk & Augustin, Hannah & Lang, Stefan. (2019). Assessing global Sentinel-2 coverage dynamics and data availability for operational Earth observation (EO) applications using the EO-Compass. *International Journal of Digital Earth*. 13. 1-17. [10.1080/17538947.2019.1572799](https://doi.org/10.1080/17538947.2019.1572799).

T. Tieng, S. Sharma, R.A. MacKenzie, M. Venkattappa, N.K. Sasaki, A. Collin Mapping mangrove forest cover using landsat-8 imagery, Sentinel-2, very high resolution images and Google earth engine algorithm for entire Cambodia IOP Conf. Ser. Earth Environ. Sci., 266 (2019), Article 012010, [10.1088/1755-1315/266/1/012010](https://doi.org/10.1088/1755-1315/266/1/012010)

Uuemaa, Evelyn; Ahi, Sander; Montibeller, Bruno; Muru, Merle; Knoch, Alexander. 2020. "Vertical Accuracy of Freely Available Global Digital Elevation Models (ASTER, AW3D30, MERIT, TanDEM-X, SRTM, and NASADEM)" *Remote Sens.* 12, no. 21: 3482. <https://doi.org/10.3390/rs12213482>

Vasquez, L.P (2019) Diseño de una metodología de clasificación de cobertura de manglar empleando imágenes SAR polarimétricas. Master thesis. Universidad Católica de Manizales. Manizales.

Voženílek V. (2009). Gramotné čtení map. *Vesmír* 88, 640, 2009/10. Dostupné z URL: <https://vesmir.cz/cz/casopis/archiv-casopisu/2009/cislo-10/gramotne-cteni-map.html>

Vozenilek, V., & Bělka, L. (2016). The Cartographic Concept of the Image Map. *ISPRS - International Archives of the Photogrammetry, Remote Sensing and Spatial Information Sciences*, 605-610.

Wang, D., Wan, B., Qiu, P., Su, Y., Guo, Q., Wang, R., Sun, F., Wu, X. 2018. Evaluating the Performance of Sentinel-2, Landsat 8 and Pléiades-1 in Mapping Mangrove Extent and Species. *Remote Sensing*, 10(1468), 2-27. <https://doi.org/10.3390/rs10091468>

Wilson AM, Jetz W (2016) Remotely Sensed High-Resolution Global Cloud Dynamics for Predicting Ecosystem and Biodiversity Distributions. *PLoS Biol* 14(3): e1002415. <https://doi.org/10.1371/journal.pbio.1002415>

Xu, Z.; Wang, Y. Radar Satellite Image Time Series Analysis for High-Resolution Mapping of Man-Made Forest Change in Chongming Eco-Island. *Remote Sens.* 2020, 12, 3438. <https://doi.org/10.3390/rs12203438>

Yancho, J. M.M.; Jones, Trevor G.; Gandhi, Samir R.; Ferster, Colin; Lin, Alice; Glass, Leah. 2020. "The Google Earth Engine Mangrove Mapping Methodology (GEEMMM)" *Remote Sens.* 12, no. 22: 3758. <https://doi.org/10.3390/rs12223758>

Zambrano, C., Rubiano, D. 1996. Mapas del bosque de manglar de la costa pacífica colombiana: años 1969, 1996 y multitemporal. Informe técnico 7. Santa fé de Bogotá: Organización Internacional de Maderas Tropicales/Ministerio del Medio Ambiente.

Zhang, X.; Tian, Q. A mangrove recognition index for remote sensing of mangrove forest from space. *Curr. Sci.* 2013, 105, 1149–1154.